

NACA TN 3974

# NATIONAL ADVISORY COMMITTEE FOR AERONAUTICS

TECHNICAL NOTE 3974

## FULL-SCALE INVESTIGATION OF SEVERAL JET-ENGINE NOISE-REDUCTION NOZZLES

By Willard D. Coles and Edmund E. Callaghan

Lewis Flight Propulsion Laboratory  
Cleveland, Ohio

LIBRARY COPY

MAR 16 1976

LANGLEY RESEARCH CENTER  
LIBRARY, NASA  
HAMPTON, VIRGINIA



Washington

FOR REFERENCE

April 1957

NOT TO BE TAKEN FROM THIS ROOM

NATIONAL ADVISORY COMMITTEE FOR AERONAUTICS

NASA Technical Library

TECHNICAL NOTE 3974

3 1176 01425 9080



FULL-SCALE INVESTIGATION OF SEVERAL JET-ENGINE

NOISE-REDUCTION NOZZLES

4363

By Willard D. Coles and Edmund E. Callaghan

SUMMARY

CN-1

A number of noise-suppression nozzles were tested on full-scale engines. In general, these nozzles achieved noise reduction by the mixing interference of adjacent jets, that is, by using multiple-slot nozzles. Several of the nozzles achieved reductions in sound power of about 5 decibels (nearly 70 percent) with small thrust losses (approx. 1 percent).

The maximum sound-pressure level was reduced by as much as 18 decibels in particular frequency bands. Some of the nozzles showed considerable spatial asymmetry, that is, the sound field was not rotationally symmetrical.

A method of calculating the limiting frequency affected by such nozzles is presented. Furthermore, data are shown which appear to indicate that further reductions in sound power will not be easily achieved from nozzles using mixing interference as a means of noise suppression.

INTRODUCTION

The normal development of the jet engine has produced sizable increases in thrust and, also, unfortunately, jet-engine noise. In fact, current jet engines are truly awesome noise producers. There are several approaches to reducing the jet-engine noise heard by the observer, that is, the public. The takeoff and climb-out pattern of the aircraft (ref. 1) can be adjusted to cause the least annoyance, or the engine itself can be made quieter.

It is well established that the principal source of jet-engine noise arises from the turbulent mixing of the jet with the surrounding atmosphere (ref. 2). The noise generated by this process is a function of the product of the eighth power of the jet velocity and the jet area (refs. 2 and 3). Consequently, reductions in jet velocity will greatly reduce

noise. To accomplish this, however, means a change in the engine cycle, for example, the bypass engine, or a completely new engine design concept, for example, the low-temperature engine (ref. 4). In any case, such a development program would require years before a reliable and tested product could be installed on new aircraft. Therefore, the present problem is to quiet existing engines.

Since the noise generation results from the turbulent mixing of the jet, a change in this process should result in a change in noise. Most of the noise-reduction devices tested during the last several years have been based on this principal. A great many different devices have been tried (refs. 5 to 7), but, in general, all seek to alter the mixing process either by odd-shaped nozzles or by the interference of multiple jets. 433

A theory relating jet turbulence to noise generation is discussed in reference 8. The most significant result of this work relates the eddy size and the turbulent intensity to noise generation. As a result of this analysis, it appears that reduction of noise generation can be accomplished in one of the following ways: (1) Eddy size is decreased at constant turbulent intensity, (2) turbulent intensity is decreased at constant eddy size, or (3), and most desirable, both eddy size and intensity are decreased. The fact that it is known how noise reduction may be accomplished helps somewhat, but it is certainly not readily apparent what physical devices will result in any of the three suggested means of noise reduction.

The devices discussed herein follow the general principles outlined for accomplishing noise reduction. Some of the devices which will be discussed have been tried elsewhere and are presented as confirmation of previous work. The investigation reported herein was conducted at the NACA Lewis laboratory as part of a long-range study of jet noise and means for its suppression.

#### SYMBOLS

The following symbols are used in this report:

A	exit area of nozzle, sq ft
$a_0$	ambient speed of sound, ft/sec
D	nozzle diameter, ft
F	engine thrust, lb
$\frac{F/\delta}{(F/\delta)_{std}}$	corrected thrust ratio

<i>f</i>	frequency, cps
<i>f<sub>x</sub></i>	frequency corresponding to <i>x</i> distance, cps
<i>h</i>	jet height (see fig. 6(b)), ft
<i>N</i>	engine speed, percent of rated rpm
<i>n</i>	number of spaces between nozzle segments
<i>P</i>	sound power of suppressor nozzle, w
<i>P<sub>std</sub></i>	sound power of standard nozzle, w
<i>s</i>	jet spacing (see fig. 6(b)), ft
<i>T</i>	tailpipe temperature, °R
<i>V</i>	jet velocity, ft/sec
<i>w</i>	jet width (see fig. 6(b)), ft
<i>x</i>	distance from nozzle exit to point at which adjacent jets impinge, ft
<i>δ</i>	ratio of engine-inlet total pressure to NACA standard sea-level pressure of 2116 lb/sq ft
<i>θ</i>	ratio of engine-inlet total temperature to NACA standard sea-level temperature of 518.7° R
<i>p<sub>0</sub></i>	atmospheric air density, slugs/cu ft

#### APPARATUS AND PROCEDURE

##### Turbojet Engines

Two axial-flow turbojet engines, with rated sea-level thrust of approximately 5,000 and 10,000 pounds, were used in this investigation. At rated conditions, the total- to static-pressure ratio across the exit nozzle was approximately 1.7 for the low-thrust engine and 2.3 for the high-thrust engine. The jet velocities were approximately 1730 and 1900 feet per second, respectively. These engines were mounted in an engine thrust stand, shown in figure 1 with the 5000-pound-thrust engine installed. The centerline of the engine is located 8 feet above the ground plane. The engines were equipped with large inlet bellmouth sections and were provided with screens at the bellmouth entrance to prevent ingestion of foreign material.

Engine thrust was measured by means of temperature-compensated strain-gage thrust links of appropriate range which gave measurements accurate to 1/2 percent. Engine airflow was measured by means of static-pressure rakes and wall taps to within 1/2 percent. Additional instrumentation was provided for measuring fuel flow, exhaust-nozzle total pressure, and jet temperature.

Three different engine exhaust cones (two larger than standard) were used with the 5000-pound-thrust engine. The larger cones were used in conjunction with the noise-suppressor nozzles. The standard cone was used only with the standard conical convergent nozzle.

4363

#### Acoustic Measurements

The thrust stand (fig. 1) is located in an area which is unobstructed rearward and to the sides for over 1/2 mile. The nearest reflecting surface, other than a small control room, was located approximately 400 feet in front of the thrust stand. The reflective effects from the control room should be extremely small at all the measuring stations shown on figure 2, because no measuring stations are close to the building and because of the small size of the building and the angle at which it is located. Measurements of the over-all sound-pressure level<sup>1</sup> were made approximately 8 feet above ground level at 15° intervals from the jet axis and at a 200-foot radius from the jet exit for all the positions shown in figure 2. Sound-pressure level was measured with a commercial sound-level meter set to a flat response from 20 to 10,000 cycles per second. Spectrum data were obtained with an automatic audiofrequency analyzer and recorder. The frequency range of this system is from 35 to 18,000 cycles per second and is divided into 27 one-third-octave bands. The spectrum recorder and related equipment were mounted in a specially adapted, insulated panel truck. Before each test, both the sound-level meter and the frequency-recording system were calibrated with a small loud-speaker-type calibrator driven by a transistor oscillator.

Although extreme care was taken to calibrate the sound-measuring equipment, other sources of error affected the results. The wind has an appreciable effect on jet direction and hence distorts the sound field. No tests were made at wind velocities greater than 14 miles per hour, but some errors do occur because of wind gusts. Tests made on different days with the same nozzle showed that local sound-pressure-level variations might be as high as  $\pm 3$  decibels because of displacement of the jet. However, the sound-power levels always varied less than  $\pm 1$  decibel. The

---

<sup>1</sup>The nomenclature of acoustic terms (sound pressure, sound-pressure level, sound power, and spectrum level) used in this report is that of reference 9.

sound power should be expected to have less error since it results from an integration over the whole sound field, and errors in local values tend to average out.

Normally acoustic measurements were made at engine rotational speeds of 100, 97.5, 92.5, and 87.5 percent of rated speed. At each engine speed, spectrum measurements required about 20 minutes. In most cases, no spectrum measurements were made at 100 percent speed.

#### Noise-Suppression Nozzles

A list of the noise-suppression nozzles used in this investigation is given in table I. For convenience, each nozzle has been assigned a letter designation (given in table I), such as "nozzle A," and so forth, and will be referred to in this manner in the succeeding discussion. Pertinent details of the nozzles are shown in figures 3 to 13.

It should be noted that area adjustment tabs have been provided at the exits of all the nozzles (e.g., fig. 3). These tabs are used to trim the exhaust area to obtain the correct relation between engine speed and tailpipe temperature, that is, rated tailpipe temperature at rated engine speed.

#### RESULTS

The effectiveness of the noise-suppression devices is demonstrated by comparison with the original noise source. Initially, comparisons will be made of the total sound power radiated, the spectrum level (sound-pressure level per cycle), and the directionality pattern for the various suppressor devices and a standard conical convergent nozzle.

Such comparisons are useful for showing trends but cannot be used as absolute measures of effectiveness since ambient conditions affect both the engine operation and the sound generation. Data will be presented for a fixed engine speed of either 97.5 or 100 percent of rated engine speed. The over-all sound-pressure levels will generally be presented for 100 percent and the spectrum level, for 97.5 percent rated engine speed for the reasons discussed in APPARATUS AND PROCEDURE. With regard to both acoustics and engine operation, final comparisons of the various nozzles will be made using normalized parameters which eliminate daily temperature and pressure variations. Furthermore, comparisons between different engines equipped with suppressor nozzles are only possible using normalized parameters.

#### Nozzle A, Six-Corrugation Nozzle

Figure 14(a) shows the directional distribution of the sound for a six-corrugation nozzle (nozzle A, fig. 3) and a standard nozzle. On this and subsequent similar figures, only one-half the total sound field is shown. The values of sound-pressure level presented are averages of the values on opposite sides of the jet axis. This has been done in order to minimize the wind effects discussed previously in APPARATUS AND PROCEDURE.

It is evident that this particular suppressor nozzle shows very little effect on the directional pattern and level of the sound. In fact, the total sound power radiated for this nozzle was 164.3 decibels as compared with 166.1 decibels for the standard nozzle. These results, in general, confirm the work of Greatrex on a similar nozzle (ref. 6). Greatrex has shown that deeper corrugations will provide greater reductions in the area of maximum sound-pressure level ( $30^\circ$  to  $60^\circ$  azimuths). Several frequency distributions of sound pressure obtained with this nozzle are shown in figure 14(b). The figure shows that the spectrum levels at azimuths of  $90^\circ$  and  $150^\circ$  are practically the same as for the standard nozzle. At a  $30^\circ$  azimuth, there is a decrease in energy between frequencies of 150 and 600 cycles per second with slight increases on either side. It is not surprising, therefore, that the power-level distribution with frequency is practically unchanged from that of the standard nozzle (fig. 14(c)).

#### Nozzle B, Three-Segment Nozzle

Nozzle B (three-segment nozzle) reflects the trend toward deeper corrugations mentioned previously (ref. 6). Figure 15(a) shows a polar plot of the over-all sound-pressure level for the three-segment nozzle (fig. 4) and the standard nozzle. It is evident from the figure that this suppressor had little effect on either directionality or sound-pressure level. Consequently, the total power radiated was reduced only slightly from that of the standard nozzle, that is, less than 1.0 decibel.

The spectrum levels (fig. 15(b)) at the  $90^\circ$  and  $150^\circ$  azimuths are quite similar to those of the standard nozzle and only that at the  $30^\circ$  azimuth shows any significant changes. Here there is a decrease in energy between frequencies of 150 and 750 cycles per second with increased values on either side. As might be expected, the frequency distribution of the sound was only slightly different from that of the standard nozzle (see fig. 15(c)).

#### Nozzle C, Twelve-Segment Nozzle with Centerbody

Nozzle C was the only one investigated on the high-thrust engine; and, as pointed out previously, the results should only be compared with

other suppressor nozzles on the basis of normalized parameters. This nozzle utilizes the idea of deep corrugations but has 12 separate segments through which the gas issues (fig. 5).

The sound polar plot of the over-all sound-pressure level for this suppressor nozzle and a standard nozzle is shown in figure 16(a). These data show a marked reduction in sound-pressure level both rearward and to the sides of the engine. In fact, the peak sound-pressure level (at the 30° azimuth) has been reduced by 11 decibels. The over-all effect has resulted in a sound-power reduction of 8.5 decibels. Most of this reduction in sound power occurred in the frequency range from 40 to 1000 cycles per second, as shown in figure 16(c). In fact, the reduction at a frequency of 200 cycles per second is about 15 decibels. Furthermore, the spectrum levels at various azimuth angles (fig. 16(b)) show quite interesting characteristics. At a 30° azimuth, the spectrum level is decreased in the frequency range between 40 and 1000 cycles per second; at a 90° azimuth, the spectrum level is decreased in the frequency range between 40 and 300 cycles per second; and at a 150° azimuth, the spectrum level is reduced in the frequency range between 40 and 2000 cycles per second.

#### Nozzle D, Nine-Section Rectangular (3 in. Wide

#### by 12 in. High) Slotted Nozzle

The effectiveness of nozzle D (9-section rectangular slotted nozzle) as a noise suppressor is shown by the polar diagram of over-all sound-pressure level (fig. 17(a)). Data are presented for the nozzle mounted both horizontally (fig. 6) and vertically. It is evident that measurements made in a horizontal plane show a different pattern, depending on nozzle orientation; hence, the usual assumption of spatial symmetry does not hold. This effect was expected, however, since the results of reference 10 for single nozzles with elongated cross sections (ellipses) show this tendency. It was expected this effect might be amplified by the use of multiple slots. The effect of nozzle orientation (fig. 17(a)) shows that the over-all sound-pressure levels increased somewhat from the 45° to the 90° azimuth and decreased from the 15° to the 30° azimuth when the nozzle was mounted vertically.

The distribution of sound pressure with frequency does not appear to differ greatly with nozzle orientation, as shown by the spectrum levels (figs. 17(b) and (c)). Aside from slight shifts in levels which reflect the results shown in figure 17(a), there are small differences in the shapes which indicate an energy shift toward higher frequencies for the nozzle mounted vertically. In essence, this means that, for a nozzle mounted horizontally, the sound pressures in the vertical plane (vertical to ground and containing the jet axis) are somewhat greater

and have more high-frequency energy than those in the horizontal plane (parallel to ground and containing the jet axis).

The fact that the sound field is not rotationally symmetrical about the jet axis means that the sound-power radiation (over-all or in frequency bands) should be calculated using average values. From the results shown in figure 17(a), it is evident that a simple arithmetic average of the intensities is sufficient to give good accuracy for either total sound power or power levels in frequency bands.

The distribution of sound power with frequency is shown in figure 17(d). It is evident that considerable decreases have been obtained at frequencies from 100 to 2000 cycles per second when compared with that of a standard nozzle. The total power radiated is 161.4 decibels as compared with 166.1 decibels for a standard nozzle.

4363

Nozzle E, Nine-Section Rectangular (2 in. Wide by  
18 in. High) Slotted Nozzle

Figure 18(a) shows the sound polar diagram for nozzle E (9-section rectangular nozzle) mounted in both the horizontal (fig. 7) and vertical positions. It is evident that the use of long narrow slots (2 by 18 in.) has resulted in considerable sound emanation at approximately right angles to the jet ( $90^\circ$  azimuth), as evidenced by the data for the vertical position. It would appear that, in general, nozzle E produces greater sound pressures than nozzle D and hence is a less-effective noise suppressor. The total sound power radiated by nozzle E is 163.9 decibels, which is 2.5 decibels more than for nozzle D but somewhat less than for the standard nozzle (166.1 db).

The distribution of sound power with frequency for nozzle E as compared with that for a standard nozzle is shown in figure 18(d). It is evident that some low-frequency energy (100 to 1500 cps) has been shifted to higher frequencies leaving the total power radiated approximately the same in both cases. It is evident from the spectrum-level curves of figures 18(b) (nozzle horizontal) and (c) (nozzle vertical) that the shift in total power spectrum results chiefly from the shift in energy in the region of maximum sound radiation ( $30^\circ$  azimuth) and the increased energy at higher frequencies for the  $90^\circ$  azimuth.

Nozzle F, Seven-Section Rectangular ( $2\frac{3}{8}$  in. Wide  
by 18 in. High) Slotted Nozzle

Nozzle F (seven-section rectangular slotted nozzle, fig. 8) is a modification of nozzle E discussed in the preceding section. The

4363  
CN-2  
original nozzle (nozzle E) was cut back and the two outer slots blocked off by an internal fairing. Both nozzle F and the original nozzle show somewhat the same characteristics. The polar diagram of over-all sound-pressure levels (fig. 19(a)) shows considerable radiation at nearly right angle to the jet axis as does the original nozzle. There is one very important difference, however. Nozzle F shows practically no effect of nozzle orientation on over-all sound-pressure level, whereas the original nozzle shows appreciable effects. It is evident from a comparison of figures 18(a) and 19(a) that nozzle F is not appreciably different from the original nozzle, E. The sound power radiated is 163.5 decibels for the modified nozzle and 163.9 decibels for the original nozzle as compared with 166.1 decibels for the standard nozzle.

The distribution of sound power for this nozzle (fig. 19(d)) shows only small differences from the original nozzle. Furthermore, the spectra at the three azimuth positions (figs. 19(b) and (c)) are quite similar to those obtained with nozzle E. At the 30° azimuth, the spectrum dip is greater for nozzle E than for nozzle F (both mounted horizontally). With vertical nozzle orientation, the reverse is true. A comparison of the spectra vertically and horizontally for nozzle F shows that, while there is spatial symmetry of the over-all sound pressure (fig. 19(a)), there is not symmetry for the individual frequency bands.

In fact, at frequencies near 1000 cycles per second (for the 30° azimuth), data for the nozzle mounted vertically (fig. 19(c)) show reductions in spectrum level (from that of the standard nozzle) of as much as 25 decibels. For the nozzle mounted horizontally (fig. 19(b)), data for the same azimuth and frequency show negligible reduction. The net effect on sound power is therefore quite small (fig. 19(d)).

#### Nozzle G, Six-Section Rectangular (6 in. Wide

#### by 9 in. High) Slotted Nozzle

The sound polar diagram for nozzle G (mounted horizontally, fig. 9) and the standard nozzle is shown in figure 20(a). There is a reduction in sound pressure for nozzle G (six-section rectangular slotted nozzle) in all directions. A check of this nozzle mounted vertically showed no appreciable changes in the sound-pressure level. The distribution of the sound power (assuming spatial symmetry) is shown in figure 20(c). Comparison of the distribution with that of the standard nozzle shows that the reduction of total power from 166.1 to 162.6 decibels results from a reduction in sound power at the frequencies below 600 cycles per second.

The spectrum-level curves (fig. 20(b)) show rather interesting characteristics when compared with those of a standard nozzle. At the

30° azimuth, there is considerable decrease in energy below frequencies of 500 cycles per second and considerable increase above frequencies of 700 cycles per second. At the 90° azimuth, the data show little effect at low frequencies but a dip in energy at frequencies between 700 and 3200 cycles per second. The results at the 150° azimuth are quite similar for both this nozzle and the standard nozzle. It is interesting that the shift in energy upward in frequency on the 30° azimuth is mostly offset by the decrease in energy above a frequency of 700 cycles per second radiated at the 90° azimuth. The resultant effect (fig. 20(c)) shows little change in the total energy above a frequency of 700 cycles per second when compared with the standard nozzle.

4  
2963

Nozzle H, Six-Section Rectangular (9 in. Wide

by 6 in. High) Slotted Nozzle

The characteristics of nozzle H (six-section rectangular slotted nozzle, fig. 10) are very similar to the characteristics of nozzle G discussed in the previous section. The total power radiated was somewhat less, 161.3 decibels compared with 162.6 decibels, and the over-all sound pressures were slightly reduced (fig. 21(a)); but, in general, the discussion given previously applies equally well for both nozzles.

Nozzle I, Six-Section Rectangular (9 in. Wide by 6 in. High)

Offset Slotted Nozzle

Nozzle I (six-section rectangular offset slotted nozzle) is a modification of the nozzle discussed in the previous section. The outer slots were cut back 6 inches and the next inner pair, 3 inches (fig. 11). Internal trimmers were used to obtain the same slot width. As might be expected, the polar diagram of sound-pressure level (fig. 22(a)), the sound power (161.4 db), and the distribution of sound power with frequency (fig. 22(c)) are nearly the same for both the modified nozzle I and the original nozzle H.

The spectrum-level curves (fig. 22(b)) show some variation from those of nozzle H, but the general trends remain the same. There is a slight shift and increase in the dip of the frequency distribution curves at a frequency of about 400 cycles per second for the 30° azimuth data. At a 90° azimuth, there is a peak in energy at a frequency of 2500 cycles per second instead of the dip obtained with the original nozzle. The total effects of these changes, however, are not large, and it would appear that the slightly noncoplanar slotted nozzle is not significantly different acoustically from the coplanar nozzle.

Nozzle J, 18-Section Rectangular ( $2\frac{3}{4}$  in. Wide by  
6 in. High) Slotted Nozzle

Sound polar diagrams for nozzle J (18-section slotted nozzle) mounted both horizontally (fig. 12) and vertically are shown in figure 23(a). It is evident that considerably higher sound-pressure levels were obtained with the nozzle mounted in the vertical position, that is, the sound field is not rotationally symmetrical. Spectrum-level curves (figs. 23(b) and (c)) for the nozzle mounted in both the horizontal and vertical positions show a considerable decrease in the low-frequency energy with some increase of high-frequency energy. This is clearly evident at the  $30^\circ$  azimuth for both nozzle orientations. The trend to less low-frequency noise is evident at both the  $90^\circ$  and  $150^\circ$  azimuths. The over-all effect is shown in figure 23(d) and indicates a 10-decibel decrease in sound pressure at a frequency of 200 cycles per second with a slight increase in the energy above a frequency of 2000 cycles per second. The total power radiated by nozzle J was 5.0 decibels less than that of the standard nozzle.

Nozzle K, 12-Section Rectangular (4 in. Wide  
by 6 in. High) Slotted Nozzle

Nozzle K (12-section rectangular slotted nozzle, fig. 13) is a modification of the 18-section slotted nozzle discussed in the previous section. The sound-pressure field obtained with this nozzle mounted horizontally is shown by the polar diagram of figure 24(a). The spectrum-level curves at three positions are shown in figure 24(b). A comparison of these results with the results for the previous nozzle do not show any significant changes, and, in fact, the 12-section nozzle appears to be a less effective suppressor. This results largely from the spectrum changes at the  $30^\circ$  azimuth in the frequency range between 300 and 1000 cycles per second (fig. 24(b)). Because this nozzle was not particularly different and not as good a suppressor as the 18-section slotted nozzle, it was not tested in the vertical position. Hence, no power levels are available since the sound field cannot be assumed rotationally symmetrical for such a configuration.

Comparison of Sound-Power Radiation by Means of Lighthill's Parameter

In order to provide a valid comparison of the sound power radiated with the various nozzles with regard to both acoustics and engine operation, the data must be normalized so that effects of daily temperature and pressure variations are insignificant. For the engine this is accomplished by properly trimming the tailpipe area such that the engine

4363

always operates with the correct relation between corrected tailpipe temperature  $T/\theta$  and corrected engine speed  $N/\sqrt{\theta}$ . It is well established (refs. 10 and 11) that the sound power radiated from a jet issuing from a circular convergent nozzle can be correlated using the Lighthill parameter  $\rho_0 A V^8 / a_0^5$ . In reference 2 it is shown that both small air-jet and full-scale engines are well correlated by a single relation if the velocity  $V$  used for the engine is defined as the ratio of engine thrust to mass flow. The linear relation of sound power and Lighthill's parameter, both in watts, was found to apply even though the nozzle pressure ratio slightly exceeded the choking value (ref. 2). Thrust losses show up as a decrease in velocity and a consequent decrease in Lighthill's parameter. This is an extremely important point since any device which reduces thrust, hence Lighthill's parameter, must show greater noise reductions than those which could be obtained by throttling back the engine (with a standard nozzle) to an equal thrust value.

Figure 25 shows the sound-power ratio (ratio of suppressor-nozzle sound power to standard-nozzle sound power) for all the nozzles plotted against Lighthill's parameter. Nozzles C, D, G, H, I, and J all give substantial reductions and, in fact, reduce the sound power by 50 to 75 percent (3 to 6 db) at rated engine power.

#### Thrust Loss of Suppressor Nozzles

As mentioned previously, conditions at the jet exit of an engine are dependent on the ambient conditions. It is well established (ref. 12) that engine thrust can be normalized by plotting corrected thrust  $F/\delta$  against corrected engine speed  $N/\sqrt{\theta}$ . Figure 26 shows the corrected thrust ratio, that is, the ratio of suppressor-nozzle corrected thrust to standard-nozzle corrected thrust, plotted as a function of corrected engine speed. It is evident there is a notable range of thrust losses. The extremely large thrust loss of nozzle F (seven-segment ( $2\frac{3}{8}$  by 18 in.) rectangular nozzle) was probably caused by low pressures acting on the surfaces between the segments. Such low pressures result from the relatively high induced velocities of the mixing air in traversing the long narrow slots between adjacent jets.

The large thrust losses of nozzle C with the large centerbody also probably result from low pressures. In this case, the hot gases separate from the cone and low pressures result. As might be expected, the thrust loss decreases at rated speed since the nozzle pressure ratio is high (2.3) and hence the flow will expand and flow farther along the cone. It is quite possible that some of this loss might be decreased by using better aerodynamic design.

It is interesting to note that nozzles G, I, and D were among the best devices tested for noise reduction, and all have quite small thrust

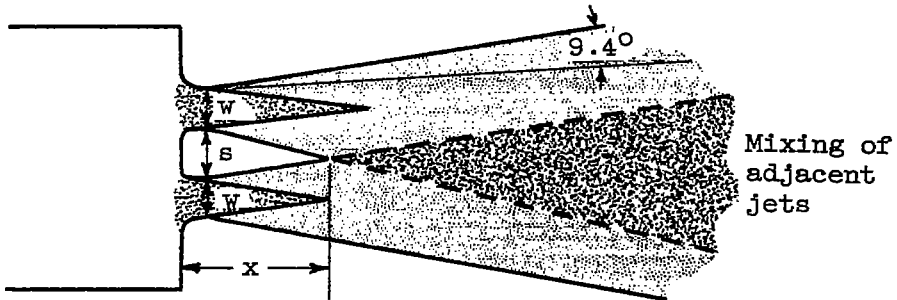
losses. Several of the data points for nozzle I are slightly greater than unity. This results from decreased pressure losses associated with the larger-than-standard exhaust cone used with this nozzle.

## DISCUSSION OF RESULTS

### Spectrum of Noise

In all cases where significant noise reduction was achieved (nozzles C, D, G, H, I, and J), the effect occurred at low frequencies. At high frequencies, the noise was either unaltered or slightly increased. For example (fig. 17(d)), nozzle D shows reduction only at frequencies less than 2400 cycles per second, while at the higher frequencies the sound-power level was virtually unchanged. The reasons for this can be explained in the following manner.

When two adjacent jets, as shown in the following sketch, emerge



from the nozzle, they mix with the surrounding air and spread. At some point downstream, the mixing zones intersect. The noise generated by each of the jets between the nozzle exit and the point of intersection should remain virtually unchanged, whereas the noise generated downstream of this point would be altered. This does not necessarily mean that the high-frequency noise (generated near the jet exit) measured in the far field would be unaltered. It would be expected that the mixing of the two jets would result in decreased eddy sizes and a consequent decrease in the low-frequency noise generated downstream with an increase in the high-frequency generation. If the turbulent intensity in the mixing region of the adjacent jets is reduced (unpublished data), then an increase in high-frequency radiation may not be too significant in terms of total sound power. This decrease in both eddy size and turbulent intensity would fulfill the requirements for noise reduction stated in reference 7.

If the adjacent jets are considered to expand uniformly at a half-angle of  $9.4^\circ$  (ref. 13), then it is possible to calculate the distance

downstream  $x$  at which the two jets impinge. It would be expected that, in general, the frequencies most affected would be those generated principally downstream of point  $x$ .

In reference 13 a curve is given of the apparent positions of the acoustic sources in a jet as a function of the axial downstream distance, the high frequencies being generated near the jet exit and the lower frequencies, downstream. These data are presented in terms of the dimensionless parameter, Strouhal number  $fD/V$ , against downstream distance in exit diameters (fig. 16, ref. 13). Unpublished NACA data show that the relation given holds over a wide range of nozzle diameters and jet velocities. If it is assumed that rectangular slots generate sound in the same manner and that the important dimension is the jet width, then it is possible to calculate the highest frequency affected by mixing interference  $f_x$ . This has been done, and the results are given in table II. These calculations were made for the conditions at a nominal engine speed of 97.5 percent rated speed. Estimates of  $f_x$  have been made for both nozzles B and C using an effective width and spacing. The effective width and spacing were calculated by assuming that, since the gas passages are roughly trapezoidal, the effective width is approximately two thirds the distance between the outer and inner shells and, of course, nearest the outer shell. No estimates were attempted for nozzle I, which has noncoplanar exits.

4  
2933

A comparison of the calculations with the frequencies estimated from the appropriate power-level distribution curves shows that, in general, the agreement is quite good. The notable exception is nozzle F. Since this nozzle was a very ineffective suppressor, the difference probably results from the dissimilarity between the actual flow conditions as compared with the simplified calculations.

#### Sound-Power Generation

Further study of the sketch shown previously would indicate that the ratio of the volume in which mixing interference occurs to the total volume of the adjacent jets is proportional to  $s/w$ . Furthermore, the volume ratio is dependent on the total number of jets for which mixing interference occurs. Since it might be expected that the outside halves of the end jets would be relatively unaffected, then the total volume ratio would be approximately the product of  $s/w$  and the number of jets less one, that is, the number of spaces between nozzle segments  $n$ . The noise suppression of the slotted nozzles would therefore be expected to be a function of  $ns/w$ .

A simple measure of the suppression of the slotted nozzles is shown by the ratio of the sound power generated by the suppressor nozzle to

4363  
that of the standard nozzle (fig. 25). Figure 27 shows this sound-power ratio (at rated engine conditions) as a function of  $ns/w$ . Also shown on this curve are the data for nozzle C, which has no end effects. The general result would appear to be that all the data except those for nozzles E, F, and J can be represented by a single curve. Undoubtedly the slot height has some effect. It would appear that this effect is small for all the nozzles except E and F. As long as there is sufficient room between adjacent jets for the mixing air to freely traverse down the slots, then the solid curve applies. If this is not the case, then the curve is shifted upward, as shown in figure 27. This upward shift probably occurs abruptly, as is usual with phenomena related to jet attachment to surfaces. Such phenomena usually occur because of a pressure differential, and the jet will try to maintain its normal pattern and then suddenly shift as a certain pressure differential is reached. From an examination of the geometry of the configurations, it would appear that this shift occurred somewhere between a spacing-to-height ratio  $s/h$  of 0.167 and 0.111.

The results for nozzle J might well be high, since this nozzle showed marked differences in the sound field dependent on the nozzle orientation. A single average of the sound powers (vertical and horizontal nozzle orientation) may not be sufficient for this particular nozzle.

It might be expected that the solid curve representing the better noise suppressors would hold generally for all suppressors of this type. In fact, unpublished data using model jets show good agreement with this curve for comparable values of jet pressure ratio. Since this is the case, then figure 27 indicates that the most noise reduction which could be expected from such suppressors occurs near  $ns/w$  of 12. It appears that further increases in  $ns/w$  will not result in substantial noise decreases. Certainly increases in  $s/w$  will tend to increase noise levels, since jets spaced far apart should be relatively unaffected by mixing interference. In fact, at large values of  $s/w$  the levels should return to that for the standard nozzle.

#### CONCLUDING REMARKS

It is evident from the results presented herein that it is possible to greatly alleviate the noise problems of current jet engines. It is not possible, however, to recommend any specific nozzle as appreciably better than all the others. Nozzles C, D, G, H, I, and J all appear to be reasonably good suppressors and reduce sound power by 50 to 75 percent (3 to 6 db). The reductions in the power in various frequency bands is as much as 15 decibels. The sound-pressure levels at particular positions showed reductions of 5 to 12 decibels with as much as 18 decibels in various frequency bands. In some cases the sound fields (nozzles D and

J) are not rotationally symmetrical and hence will cause special problems. Nozzles C, H, and J had considerable thrust loss (about 4 to 7 percent), whereas nozzles D, G, and I had quite small thrust losses.

Apparently it is not possible to achieve a great deal more sound reduction from the types of nozzles presented herein. The conversion of the test nozzles to flying hardware represents a considerable development effort. Furthermore, a great many practical problems in regard to nozzle weight and drag in flight remain to be answered. Certainly all the nozzles tested will require further study to minimize these effects.

#  
293

Lewis Flight Propulsion Laboratory  
National Advisory Committee for Aeronautics  
Cleveland, Ohio, January 22, 1957

#### REFERENCES

1. North, Warren J.: Effect of Climb Technique on Jet-Transport Noise. NACA TN 3582, 1956.
2. Coles, Willard D., and Callaghan, Edmund E.: Investigation of Far Noise Field of Jets. II - Comparison of Air Jets and Jet Engines. NACA TN 3591, 1956.
3. Lighthill, M. J.: On Sound Generated Aerodynamically. I - General Theory. Proc. Roy. Soc. (London), ser. A., vol. 211, no. 1107, Mar. 20, 1952, pp. 564-587.
4. Silverstein, Abe, and Sanders, Newell D.: Concepts on Turbojet Engines for Transport Application. Preprint No. 727, SAE, 1956.
5. Tyler, John, and Towle, George: A Jet Exhaust Silencer. Preprint No. 508, SAE, 1955.
6. Greatrex, F. B.: Jet Noise. Preprint No. 559, Inst. Aero. Sci., June 1955.
7. Withington, Holden W.: Silencing the Jet Aircraft. Aero. Eng. Rev., vol. 15, no. 4, Apr. 1956, pp. 56-63; con't., p. 84.
8. Sanders, Newell D., and Laurence, James C.: Fundamental Investigation of Noise Generation by Turbulent Jets. Preprint No. 744, SAE, 1956.

- 4363  
CN-3
9. Bolt, R. H., Lubasik, S. J., Nolle, A. W., and Frost, A. D., eds.: Handbook of Acoustic Noise Control. Vol. 1. Physical Acoustics. WADC Tech. Rep. 52-204, Aero. Medical Lab., Wright Air Dev. Center, Wright-Patterson Air Force Base, Dec. 1952. (Contract No. AF 33(038)-20572, RDO No. 695-63.)
  10. Callaghan, Edmund E., and Coles, Willard D.: Investigation of Far Noise Field of Jets. I - Effect of Nozzle Shape. NACA TN 3590, 1956.
  11. Tyler, John M., and Perry, Edward C.: Jet Noise. Preprint No. 287, SAE, 1954.
  12. Sanders, Newell D.: Performance Parameters for Jet-Propulsion Engines. NACA TN 1106, 1946.
  13. Howes, Walton L., and Mull, Harold R.: Near Noise Field of a Jet-Engine Exhaust. I - Sound Pressures. NACA TN 3763, 1956.

TABLE I. - NOISE-SUPPRESSION NOZZLES

Letter designation	Rated thrust of test engine, lb	Description of nozzle	Details in fig. -
A	5,000	Six-corrugation or Greatrex type (ref. 6) nozzle	3
B	5,000	Three-segment-nozzle	4
C	10,000	Twelve-segment nozzle with centerbody	5
D	5,000	Nine-section rectangular (3 in. wide by 12 in. high) slotted nozzle	6
E	5,000	Nine-section rectangular (2 in. wide by 18 in. high) slotted nozzle	7
F	5,000	Seven-section rectangular ( $2\frac{5}{8}$ in. wide by 18 in. high) slotted nozzle (modification of nozzle E)	8
G	5,000	Six-section rectangular (6 in. wide by 9 in. high) slotted nozzle	9
H	5,000	Six-section rectangular (9 in. wide by 6 in. high) slotted nozzle	10
I	5,000	Six-section rectangular (9 in. wide by 6 in. high) offset (different exit planes) slotted nozzle	11
J	5,000	Eighteen-section rectangular (2.7 in. wide by 6 in. high) slotted nozzle	12
K	5,000	Twelve-section rectangular (4 in. wide by 6 in. high) slotted nozzle (modification of nozzle J)	13

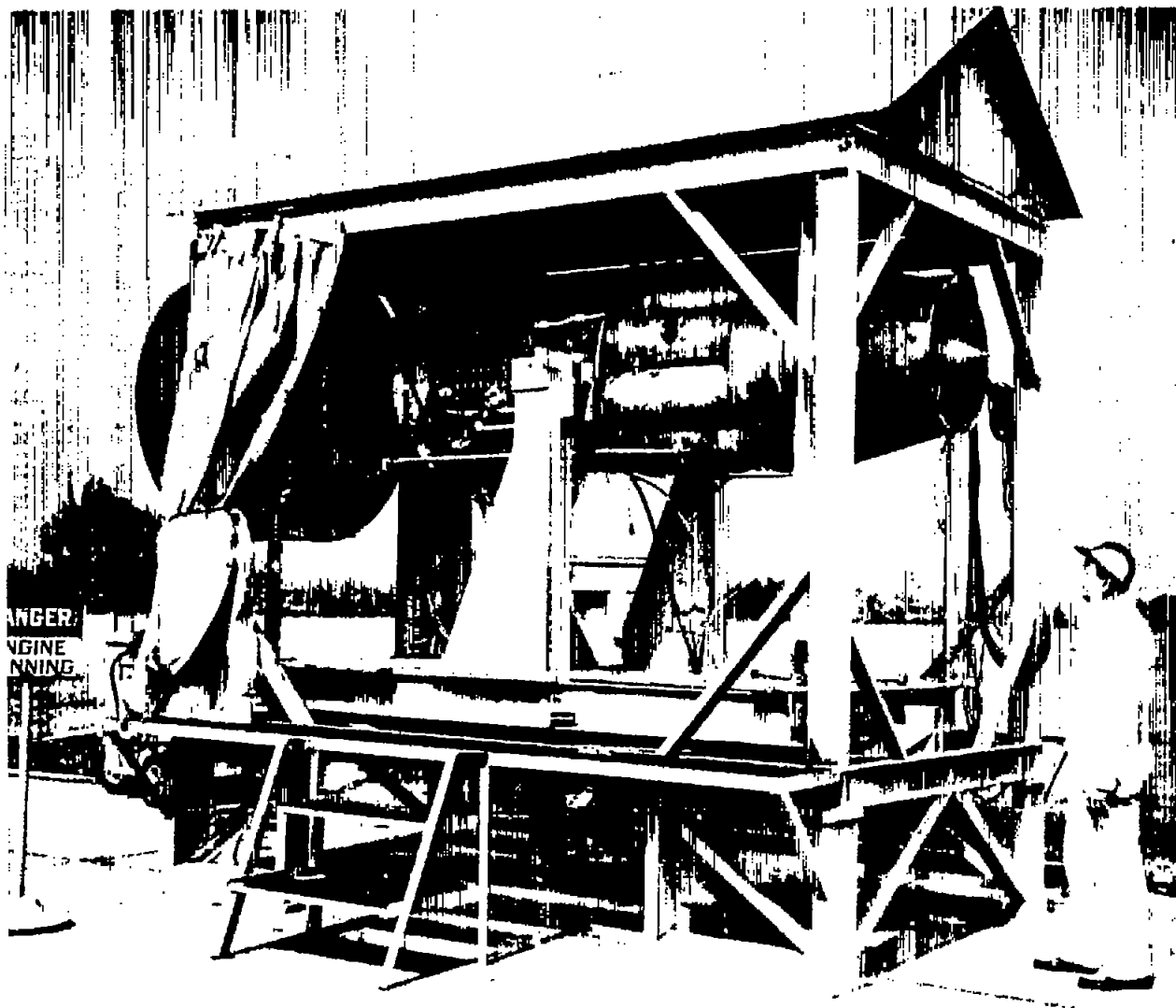
4363

TABLE II. - FREQUENCY  $f_x$  AT DISTANCE  $x$ 

DOWNSTREAM WHERE ADJACENT JETS IMPINGE

Nozzle	$f_x$ , cps	
	Calculated	Measured
B	1223	1000 (fig. 14(c))
C	1365	1600 (fig. 15(c))
D	2600	2400 (fig. 16(d))
E	1815	1800 (fig. 17(d))
F	3170	2200 (fig. 18(d))
G	914	720 (fig. 19(c))
H	850	800 (fig. 20(c))
J	2270	2100 (fig. 22(d))

NACA TN 3974



C-43077

Figure 1. - Thrust stand with 5000-pound-thrust engine.

4363

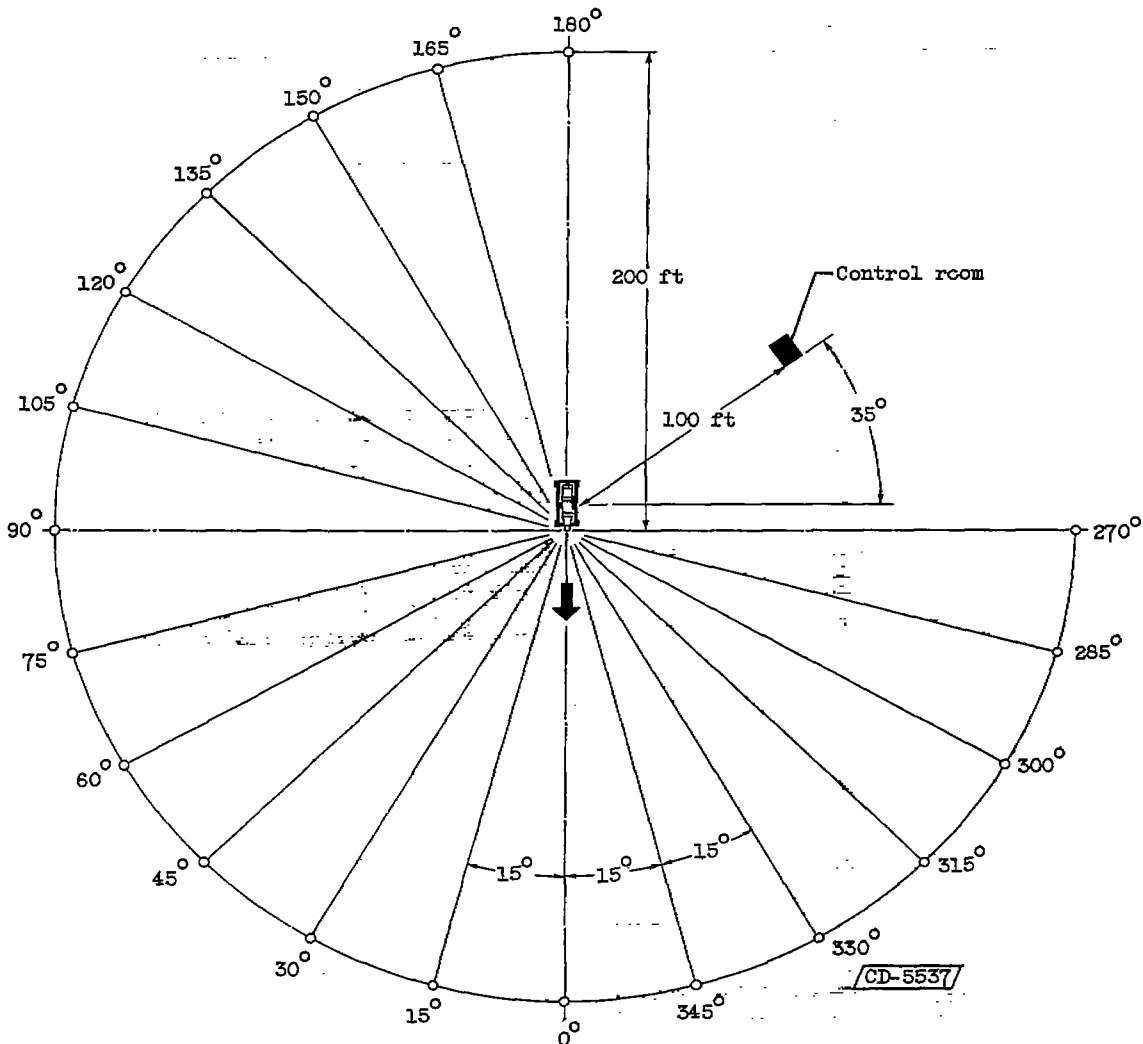
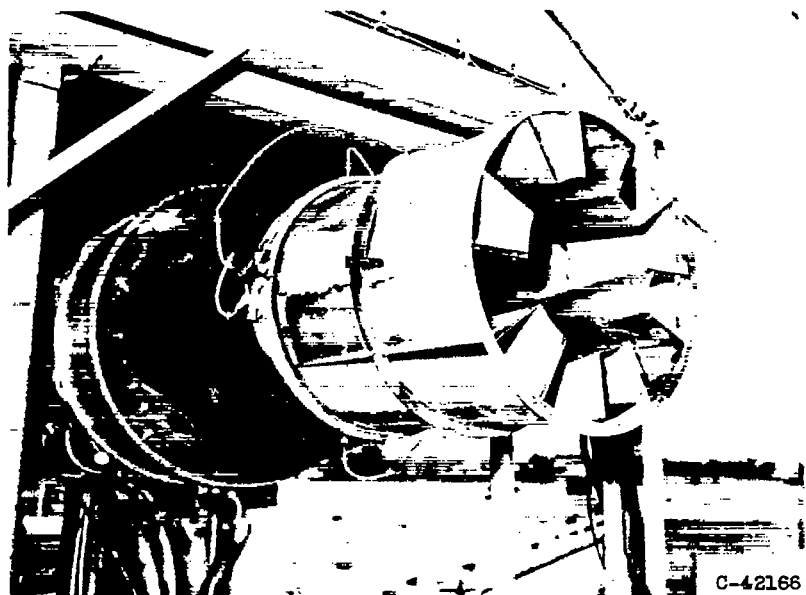
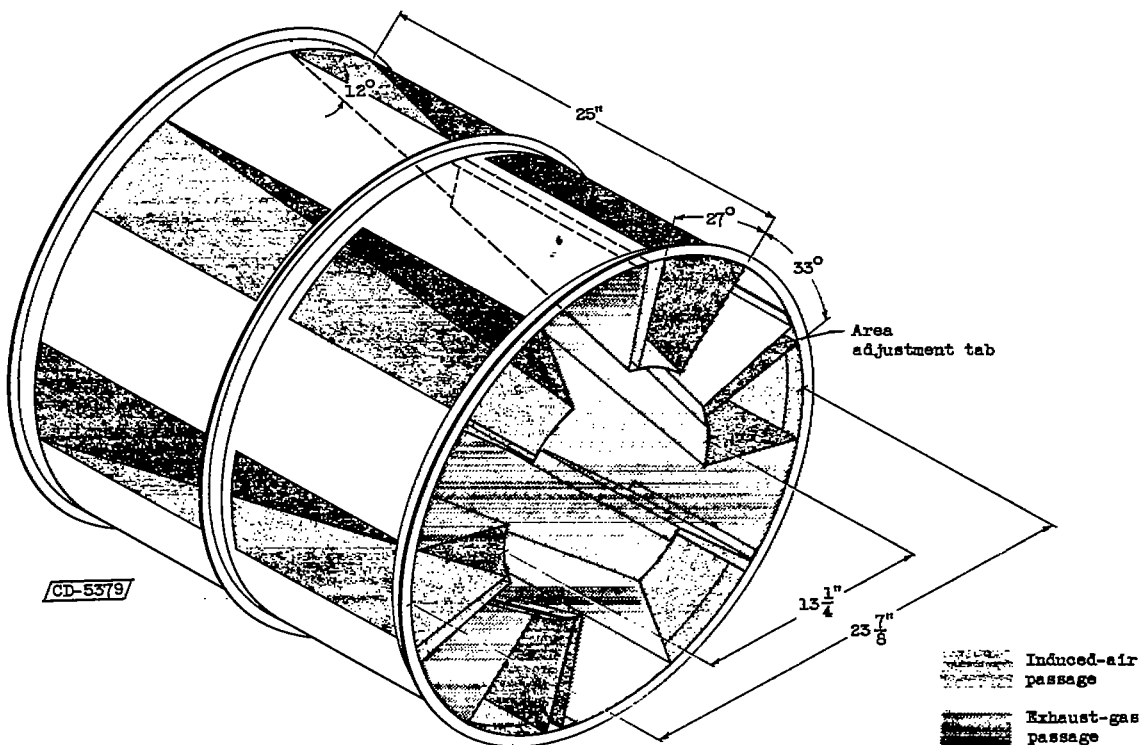


Figure 2. - Location of survey stations in sound field around engine thrust stand.

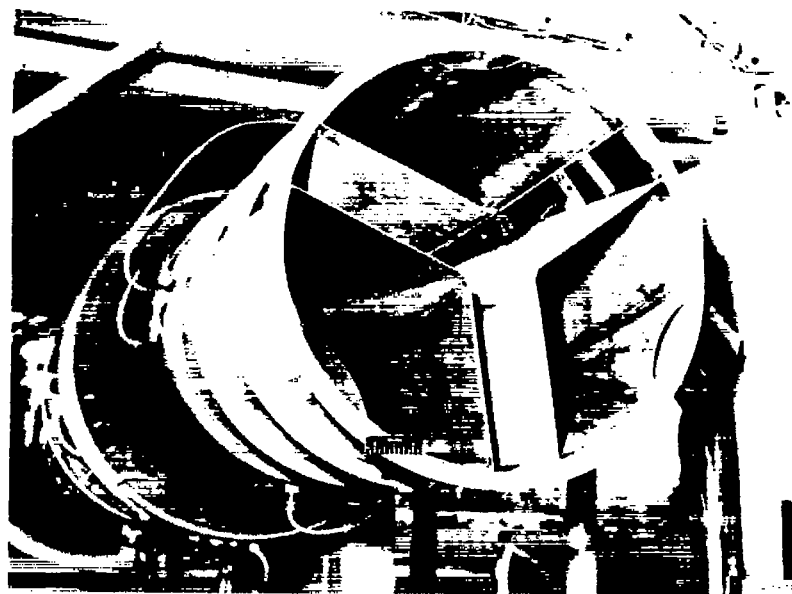


(a) Photograph.



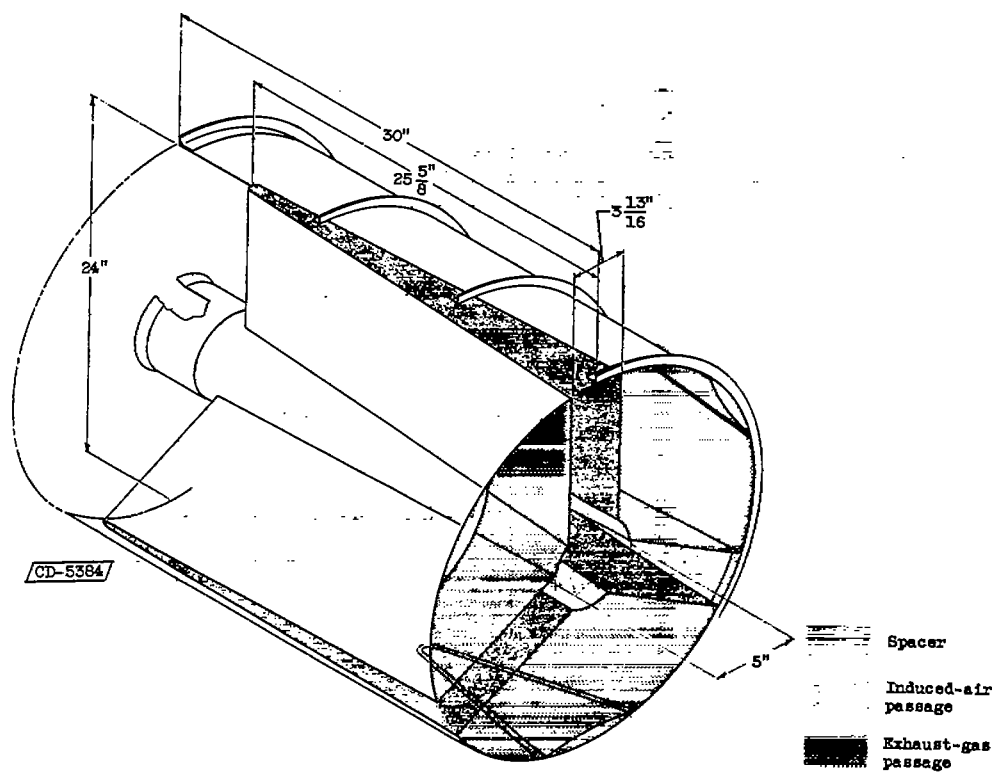
(b) Sketch.

Figure 3. - Nozzle A, six-corrugation or Greatrex type (ref. 6) nozzle.



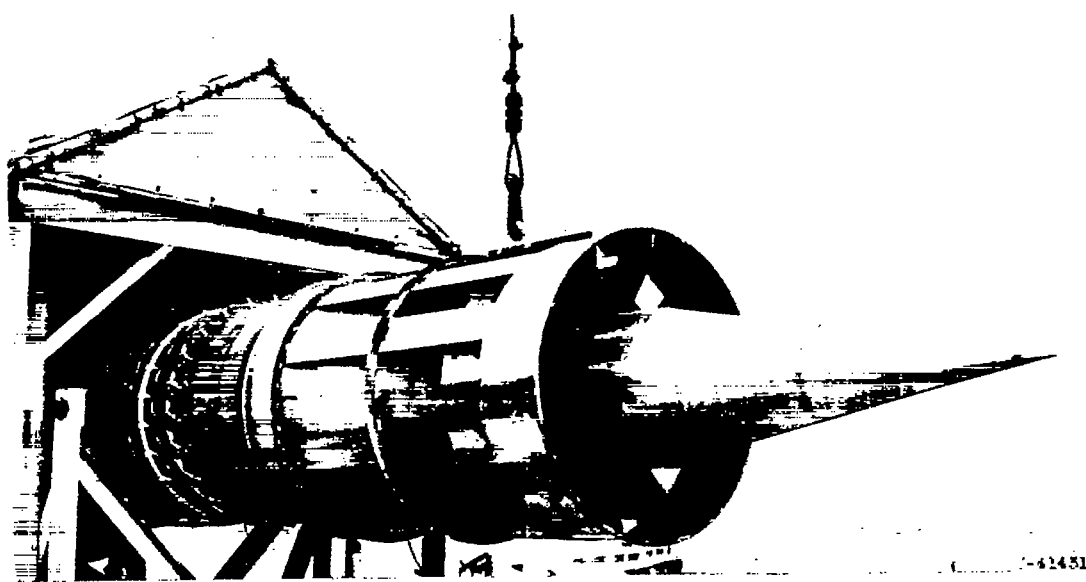
CQCR#

(a) Photograph.

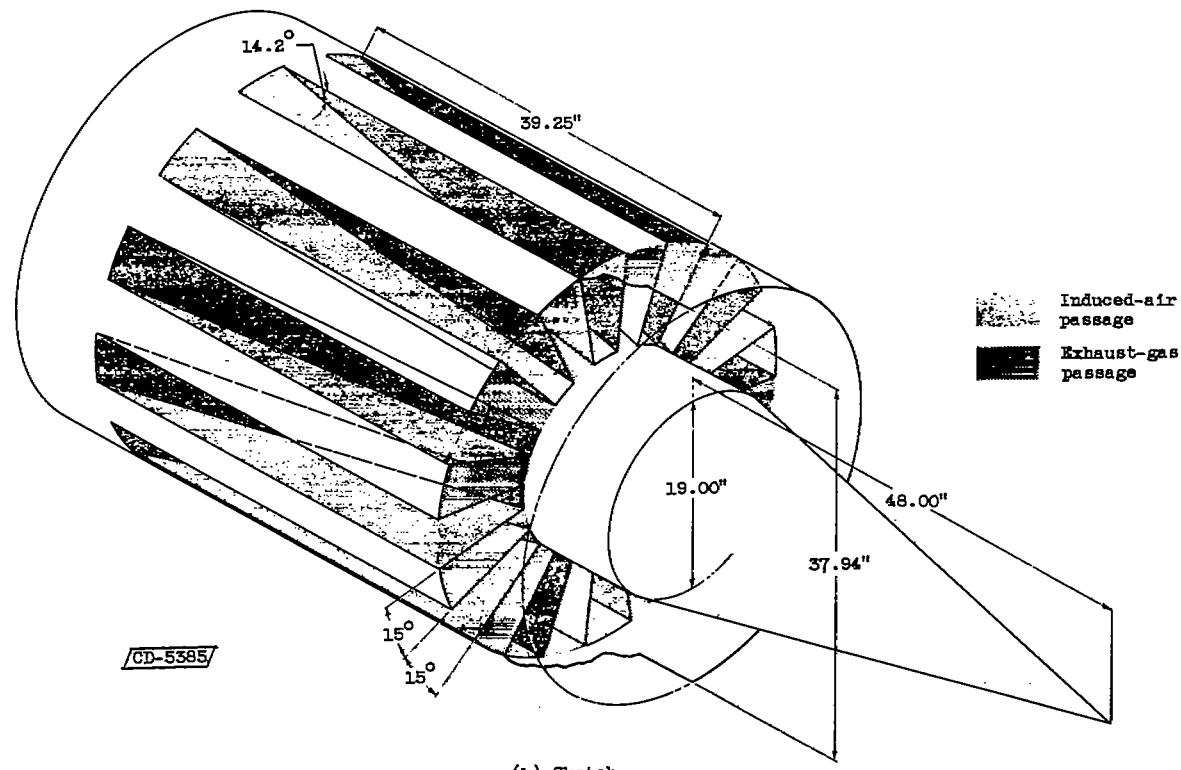


(b) Sketch.

Figure 4. - Nozzle B, three-segment nozzle.

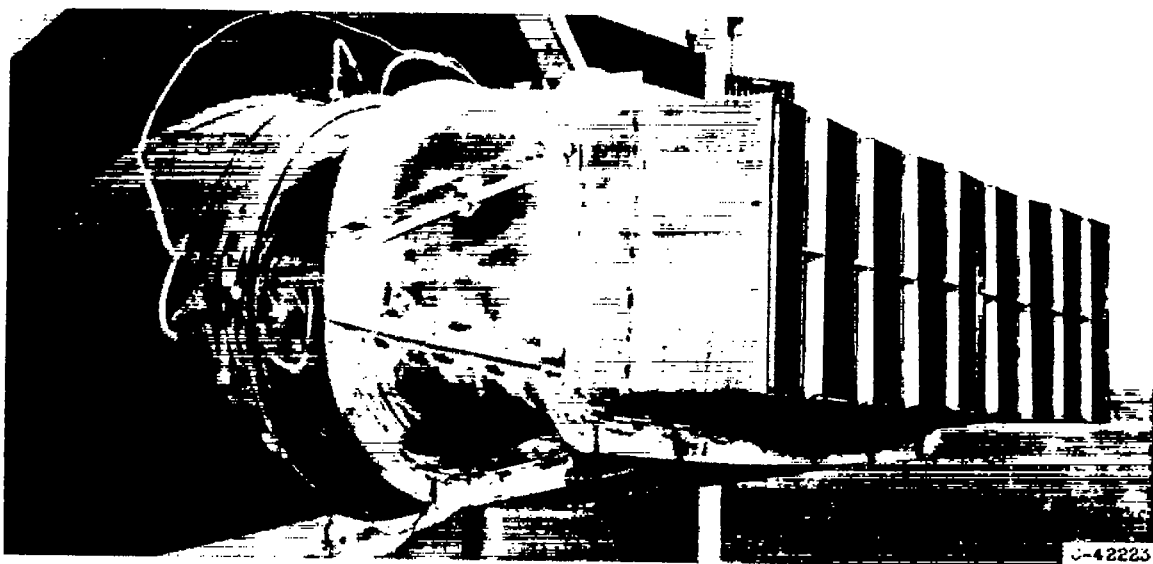


(a) Photograph.

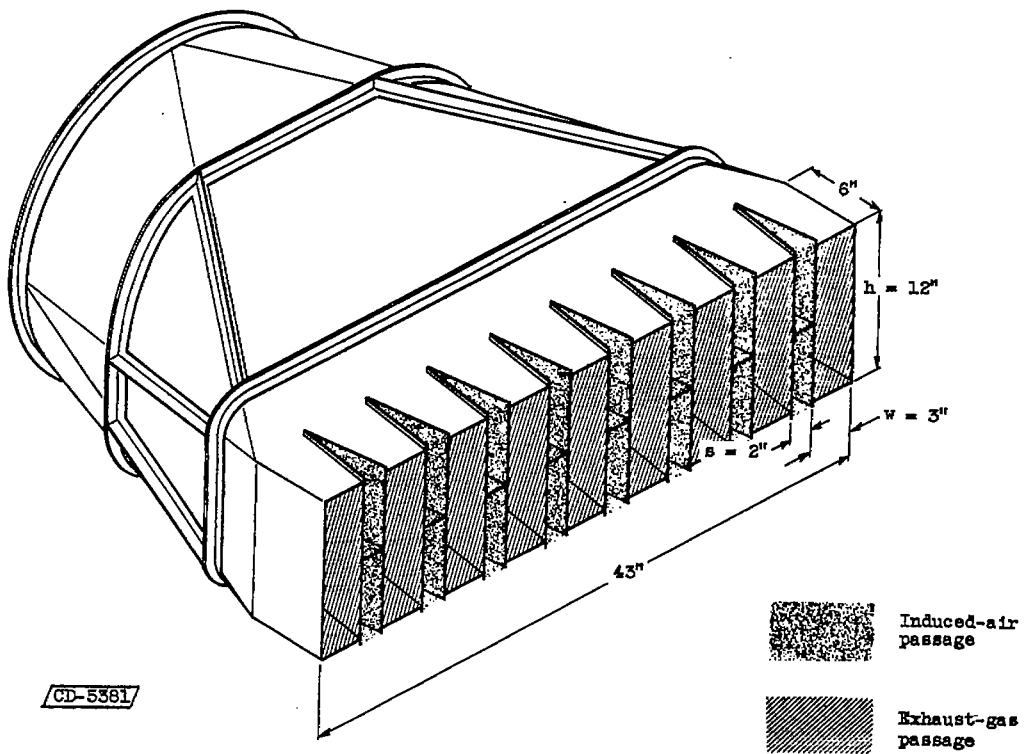


(b) Sketch.

Figure 5. - Nozzle C, twelve-segment nozzle with centerbody.



(a) Photograph.

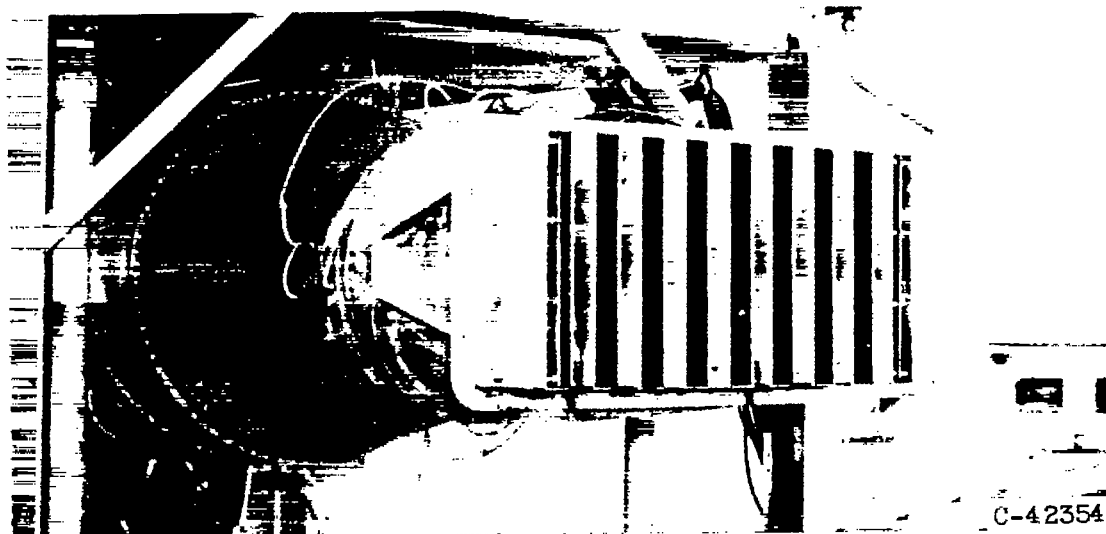


(b) Sketch.

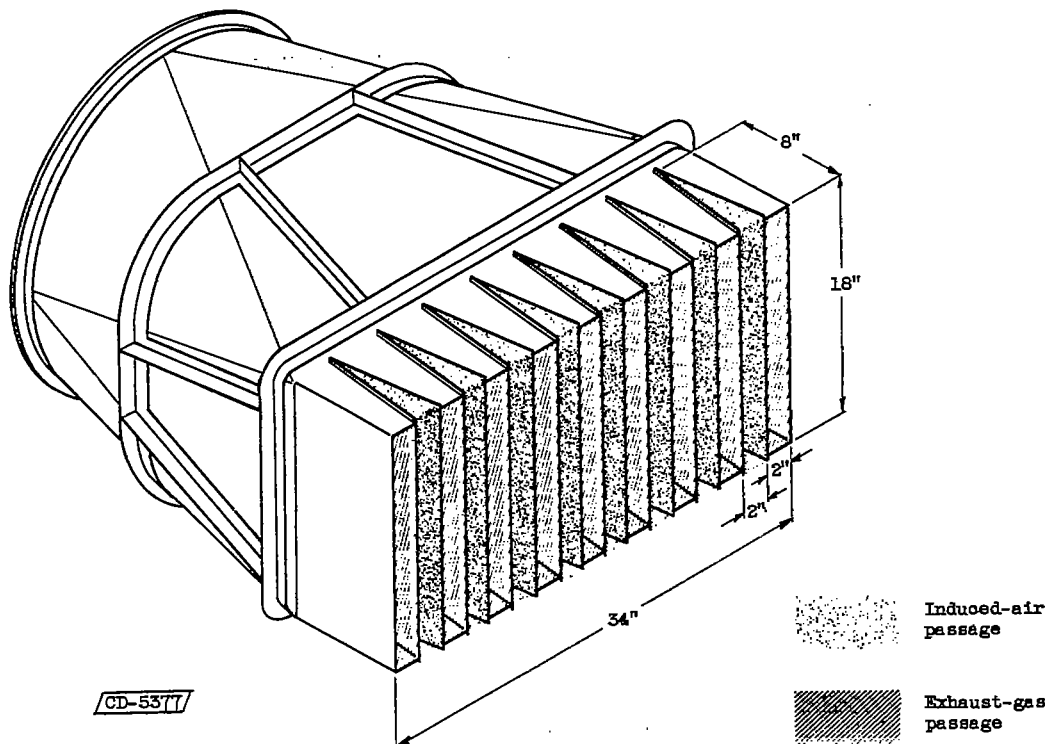
Figure 6. - Nozzle D, nine-section rectangular (3 in. wide by 12 in. high) slotted nozzle.

4363

CN-4



(a) Photograph.



(b) Sketch.

Figure 7. - Nozzle E, nine-section rectangular (2 in. wide by 18 in. high) slotted nozzle.

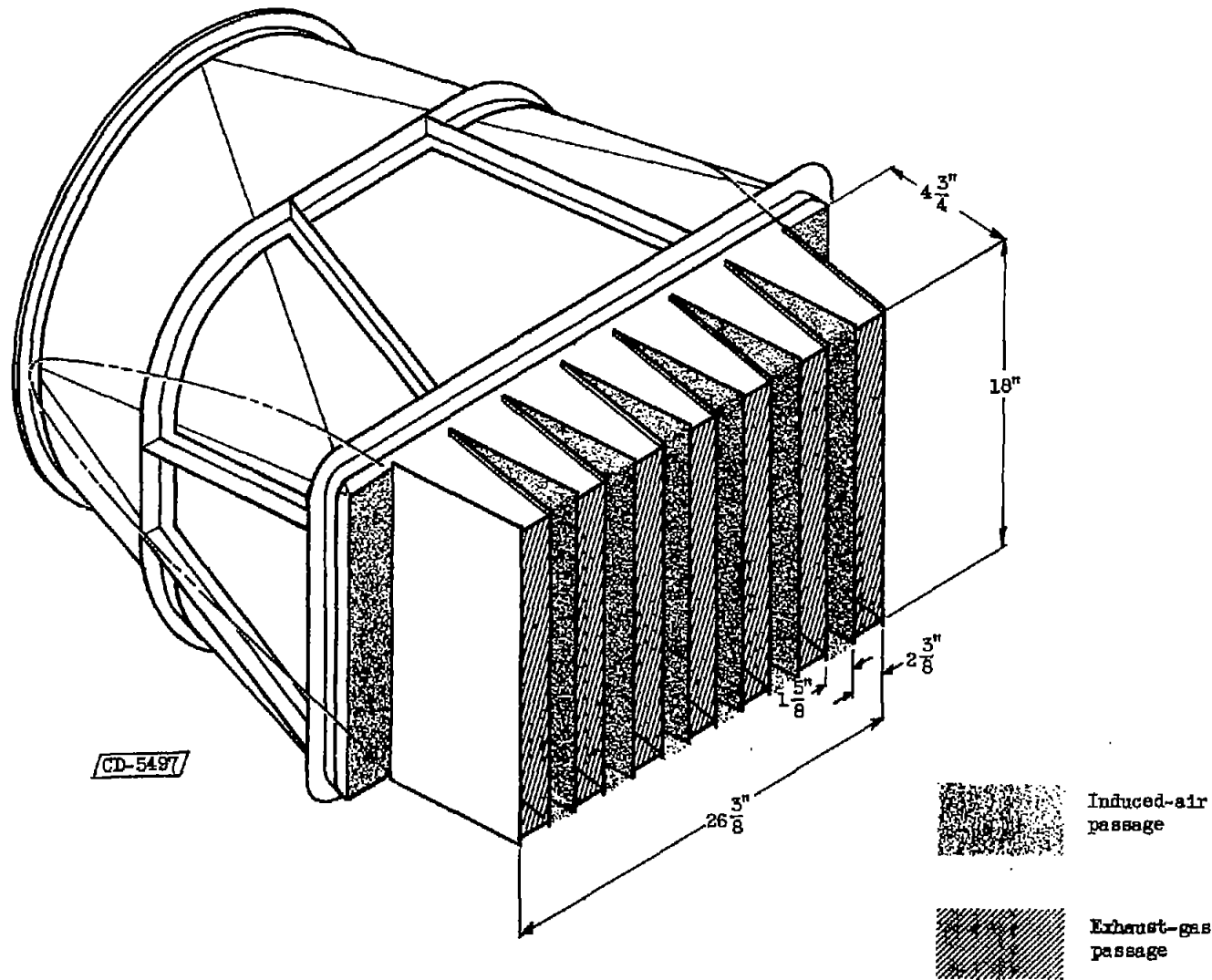
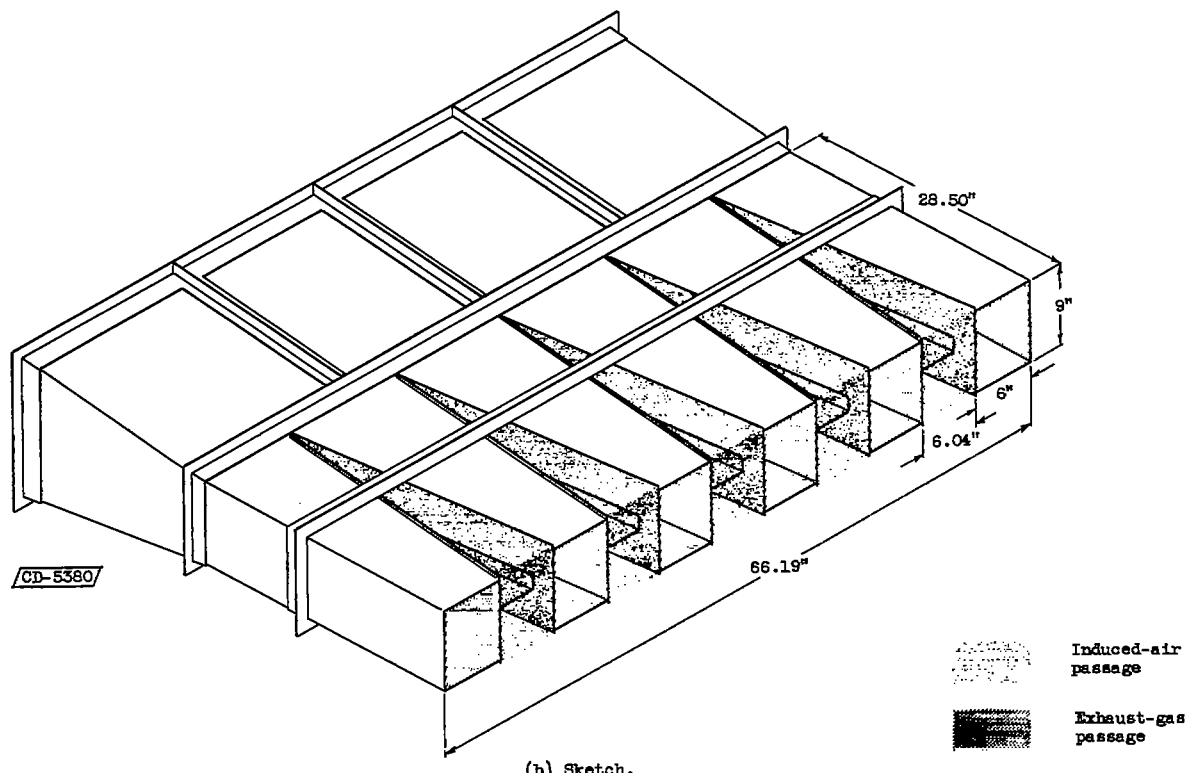


Figure 8. - Nozzle F, seven-section rectangular ( $2\frac{5}{8}$  in. wide by 18 in. high) slotted nozzle.

CN-4 back  
4363

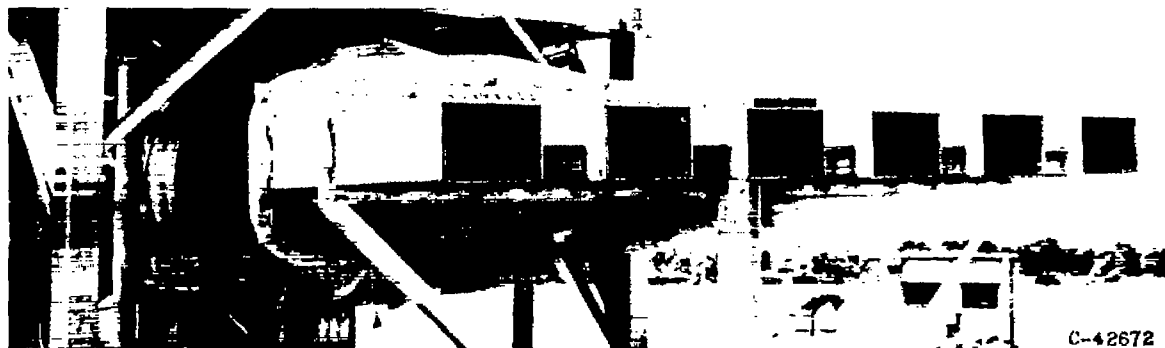
(a) Photograph.



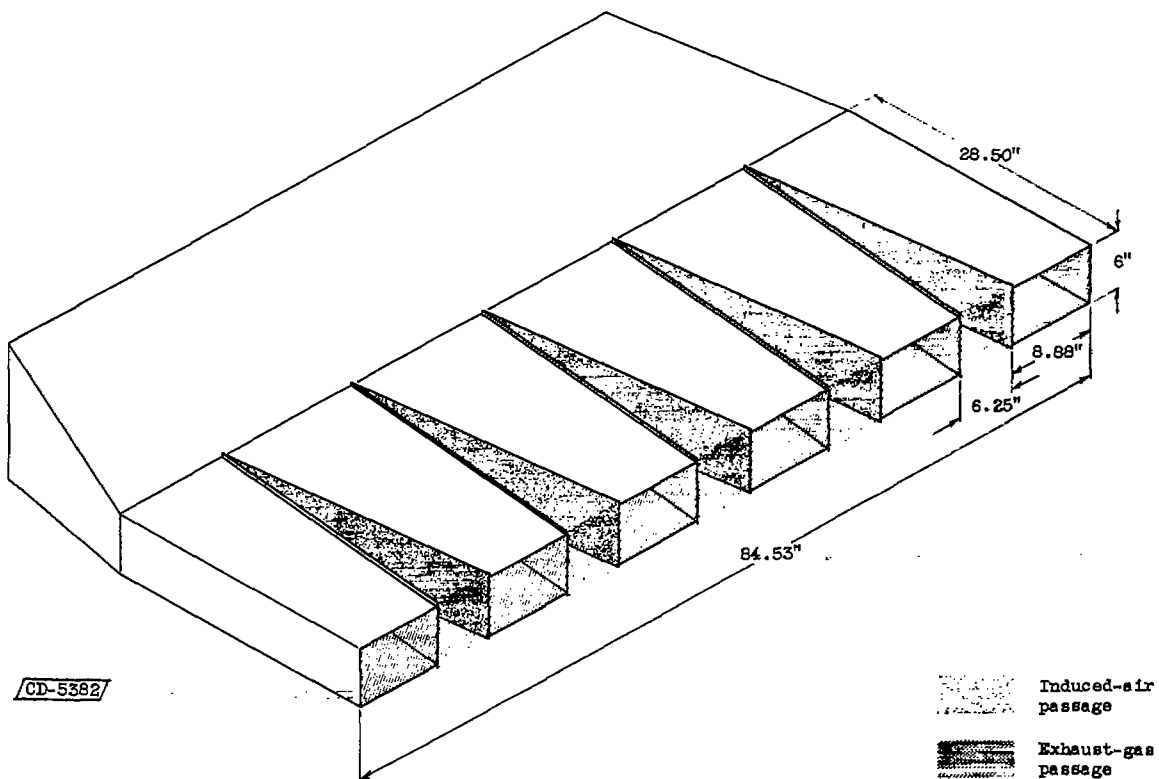
(b) Sketch.

Figure 9. - Nozzle G, six-section rectangular (6 in. wide by 9 in. high) slotted nozzle.

4363

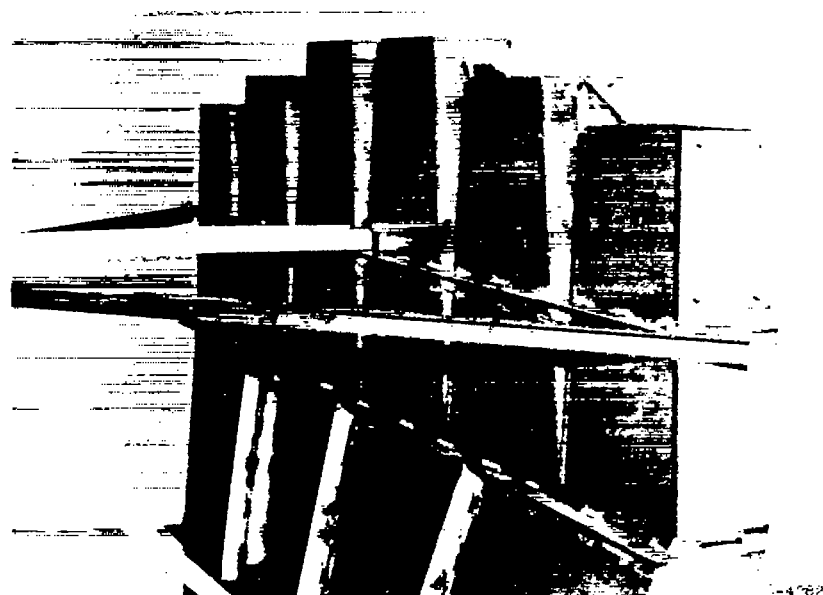


(a) Photograph.

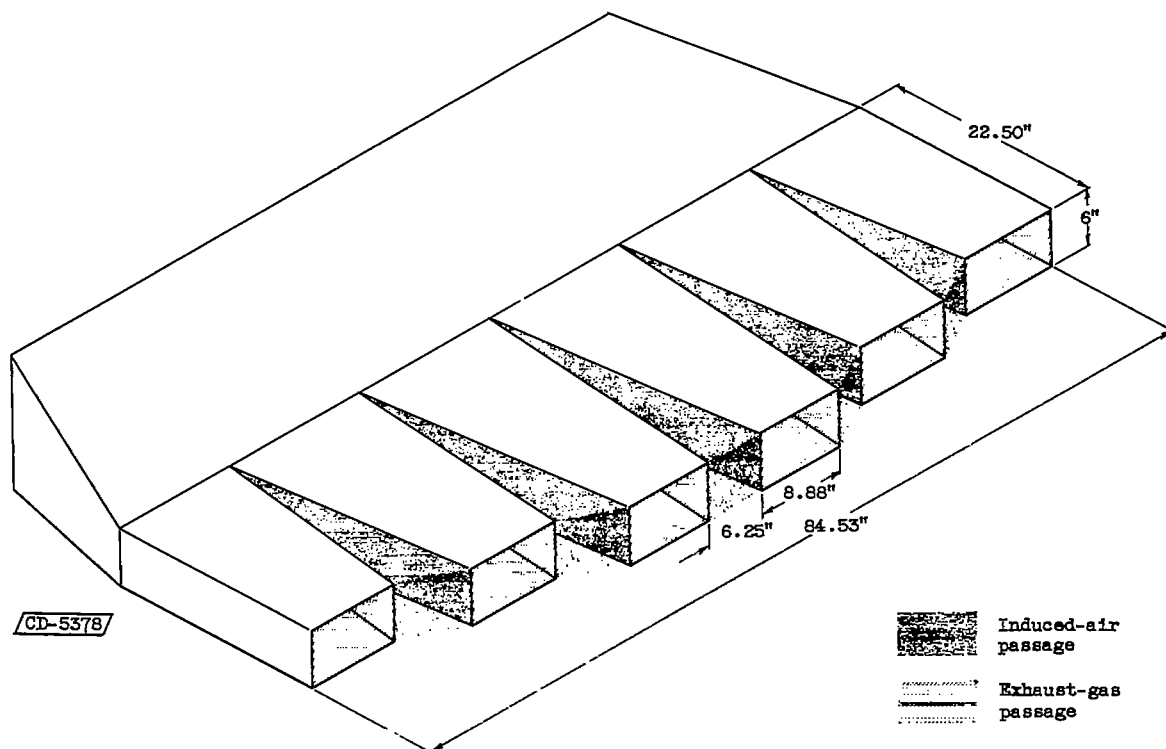


(b) Sketch.

Figure 10. - Nozzle H, six-section rectangular (9 in. wide by 6 in. high) slotted nozzle.



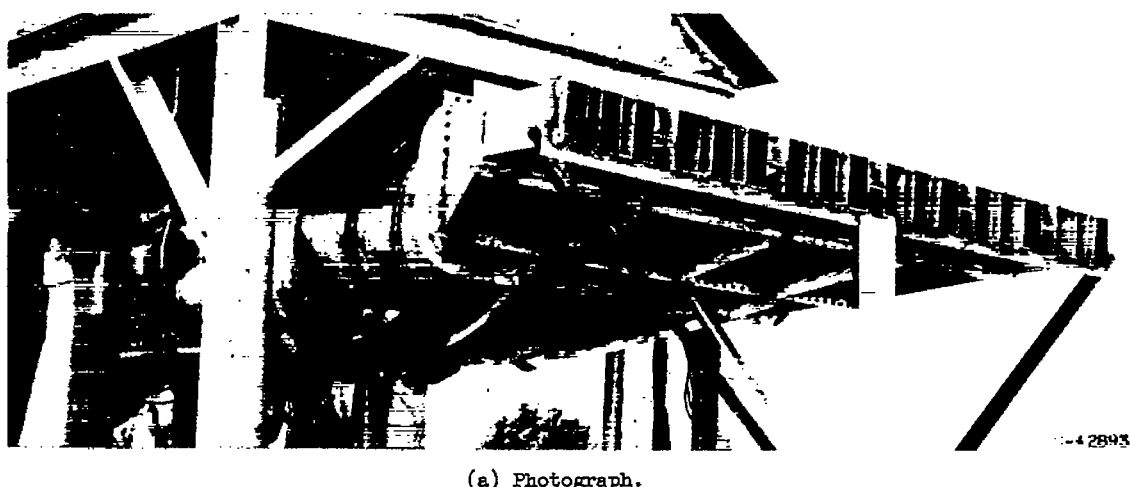
(a) Photograph.



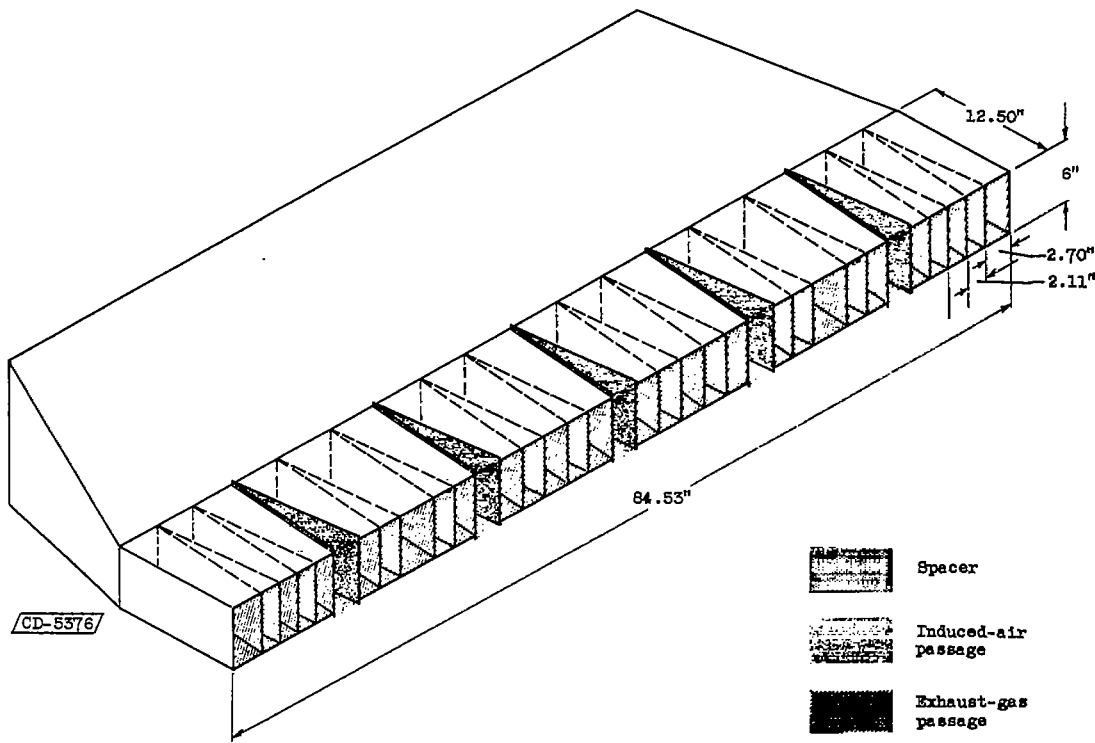
(b) Sketch.

Figure 11. - Nozzle I, six-section rectangular (9 in. wide by 6 in. high) offset slotted nozzle.

436C



(a) Photograph.



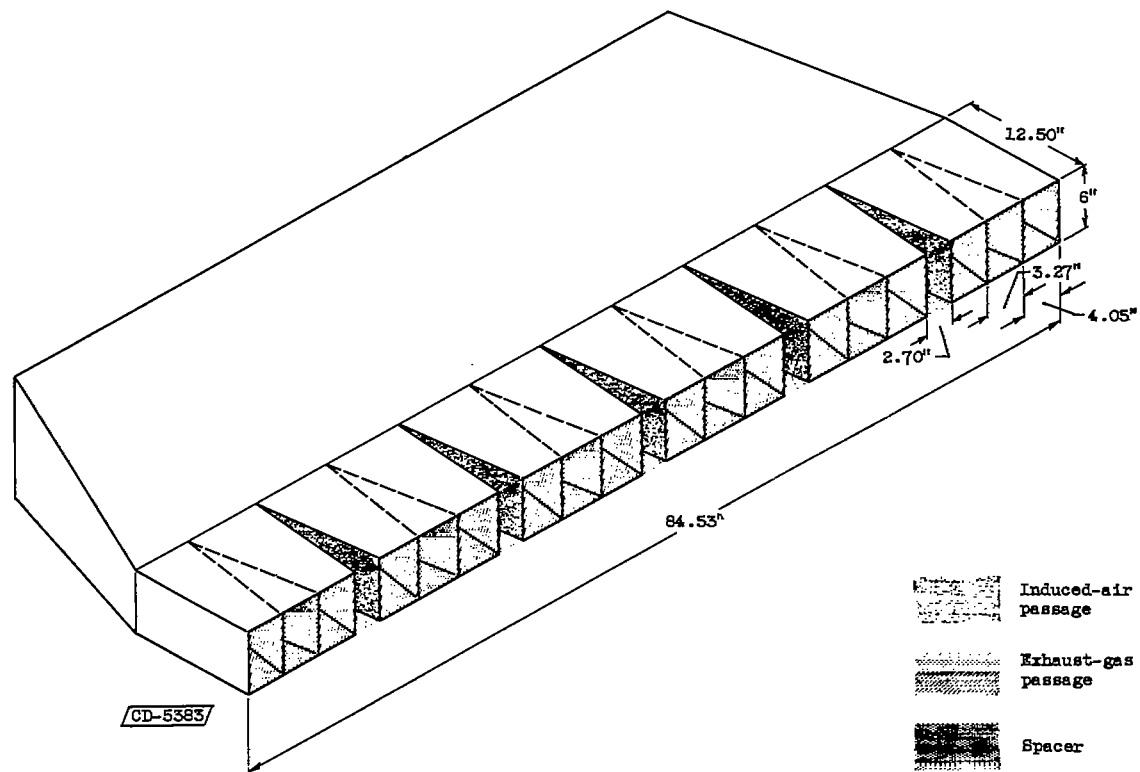
(b) Sketch.

Figure 12. - Nozzle J, eighteen-section rectangular (2.7 in. wide by 6 in. high) slotted nozzle.

4563



(a) Photograph



(b) Sketch.

Figure 13. - Nozzle K, twelve-section rectangular (4 in. wide by 6 in. high) slotted nozzle.

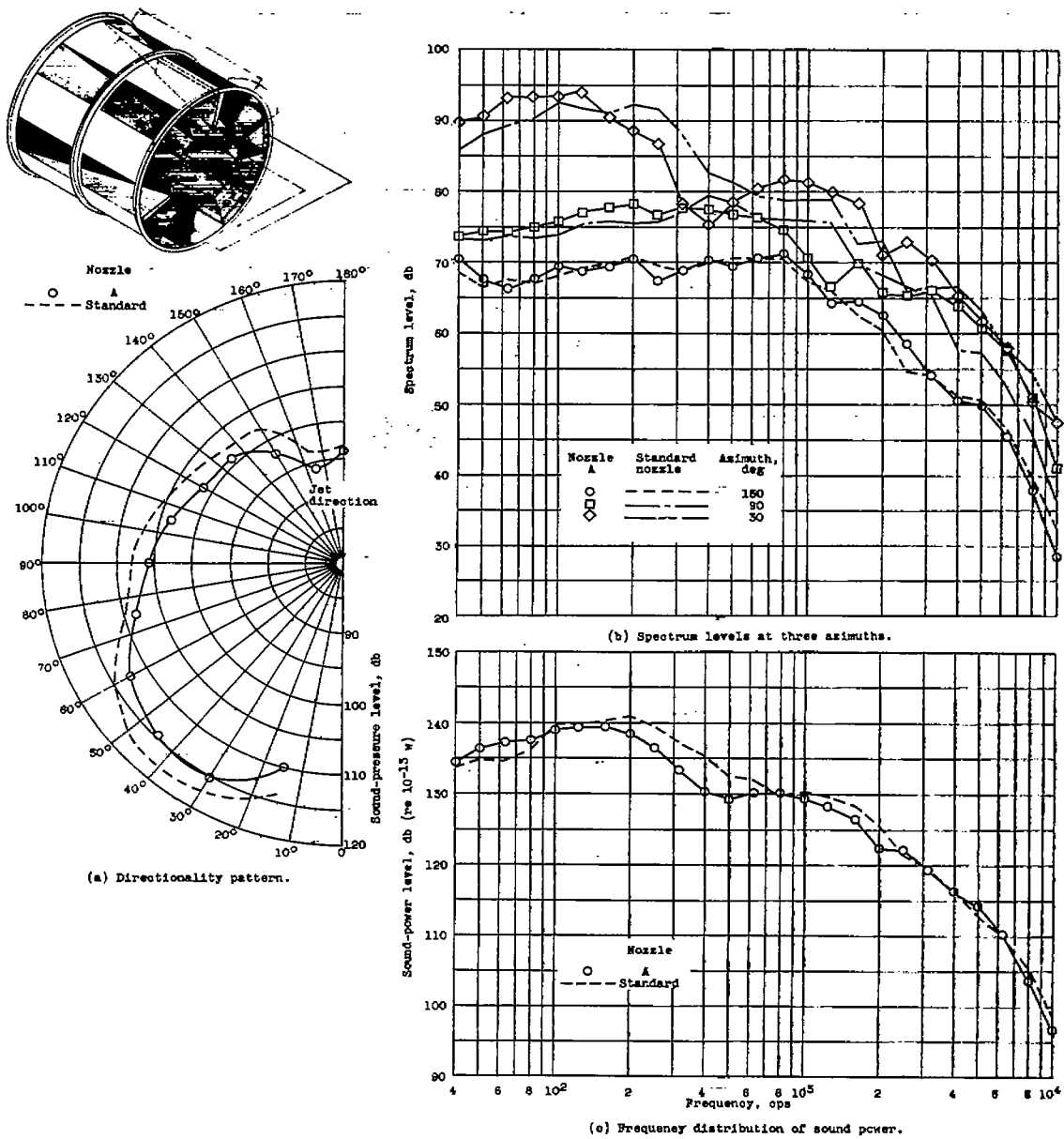


Figure 14. - Sound-field characteristics of nozzle A.

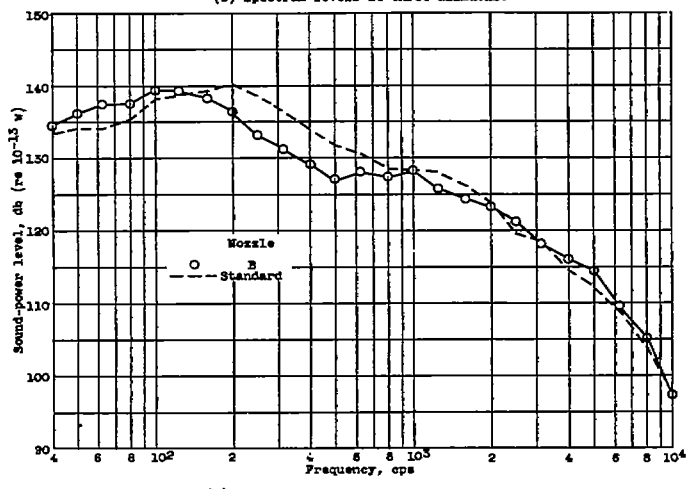
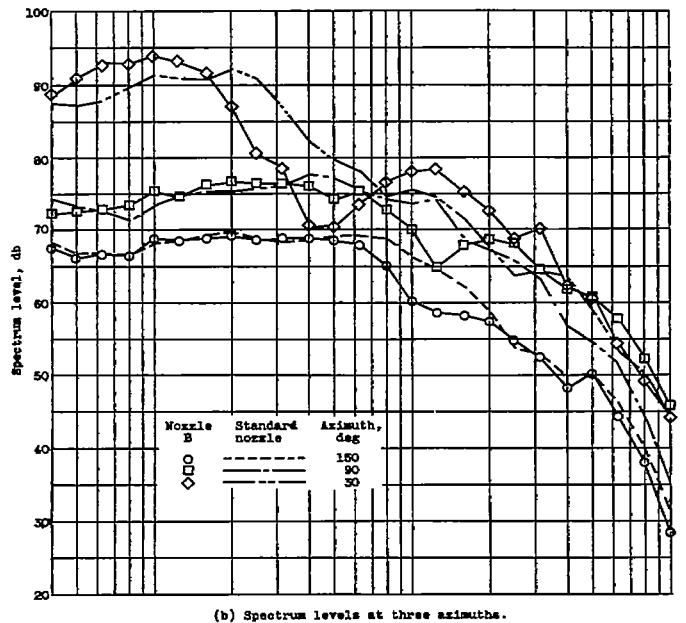
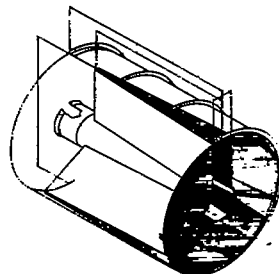
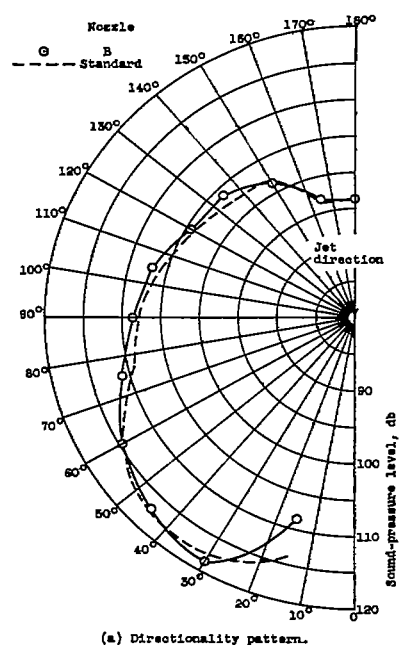


Figure 15. - Sound-field characteristics of nozzle B.

4762

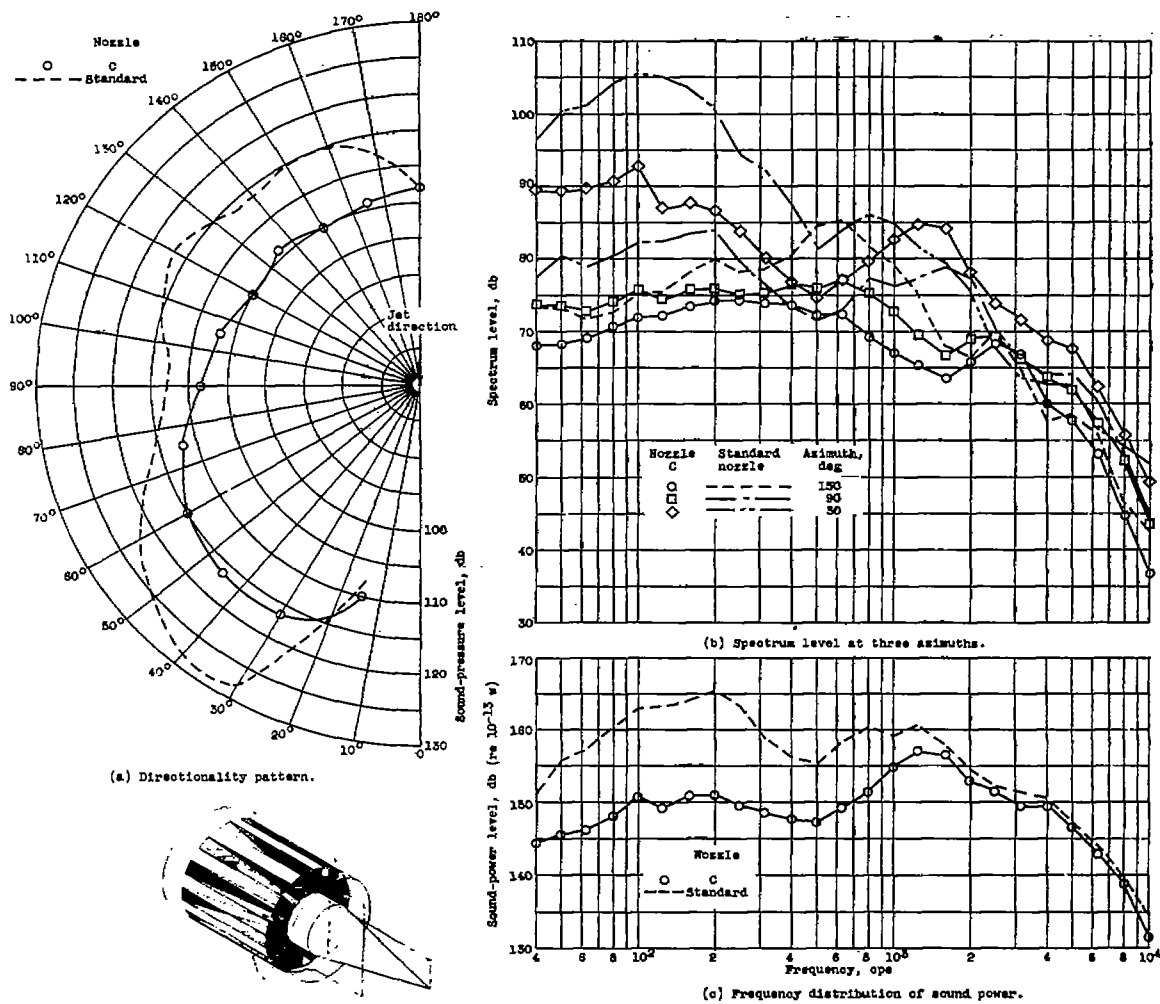
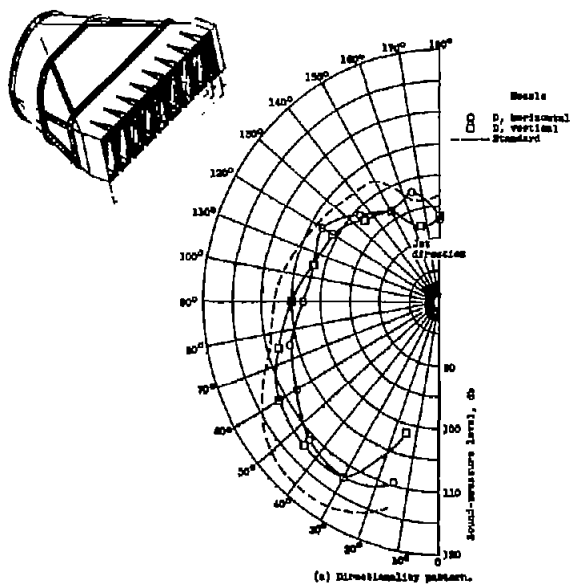
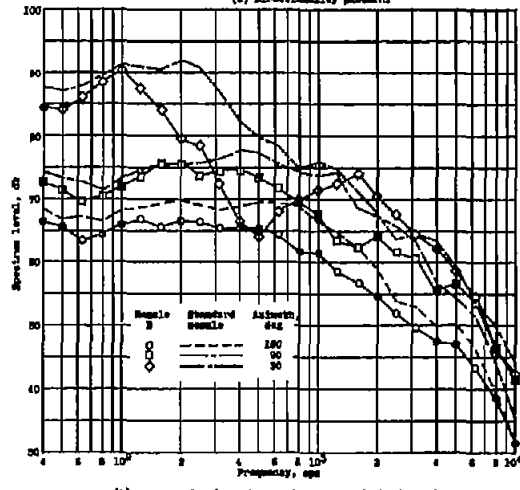


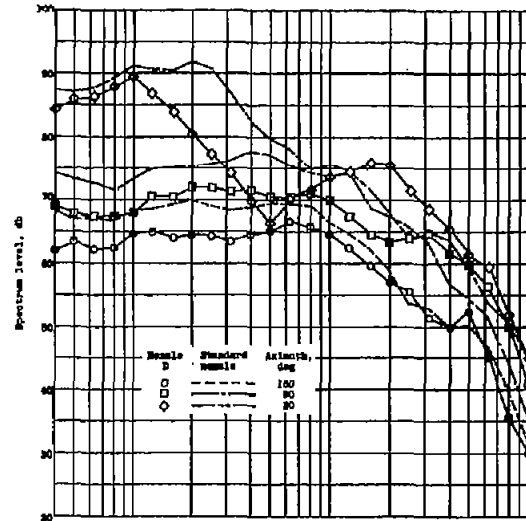
Figure 16. - Sound-field characteristics of nozzle C.



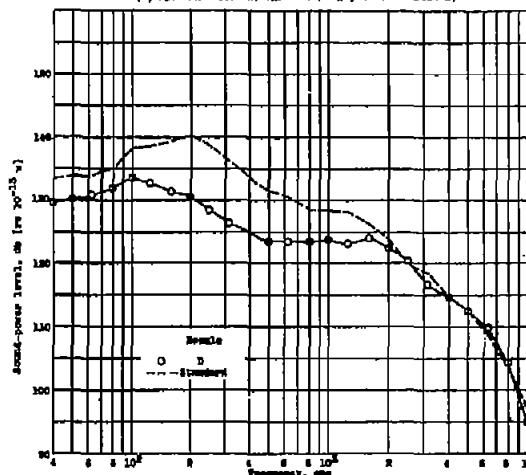
(a) Directivity pattern.



(b) Spectrum level at three azimuths, nozzle horizontal.



(c) Spectrum level at three azimuths, nozzle vertical.



(d) Frequency distribution of sound power.

Figure 17. - Sound-field characteristics of nozzle D.

4363

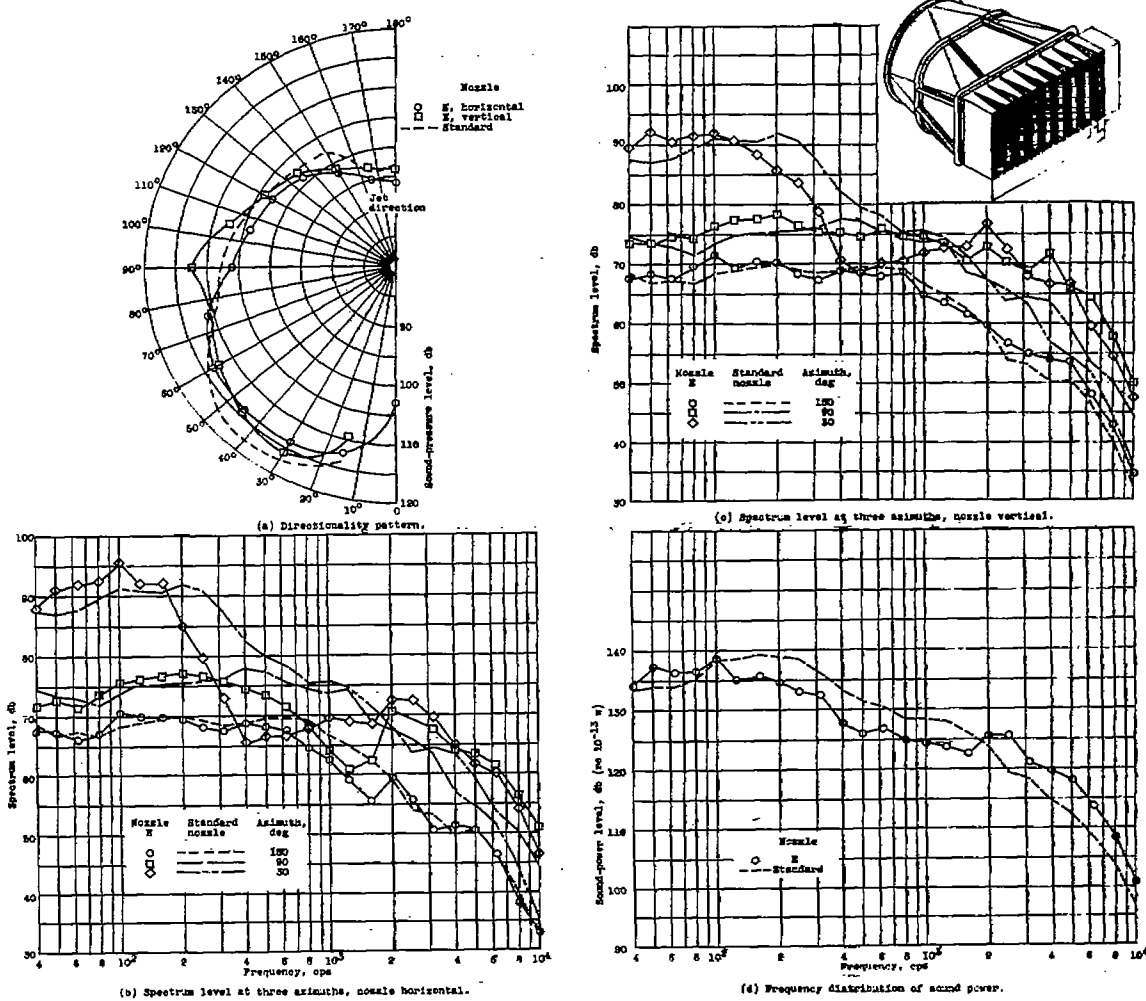


Figure 18. - Sound-field characteristics of nozzle E.

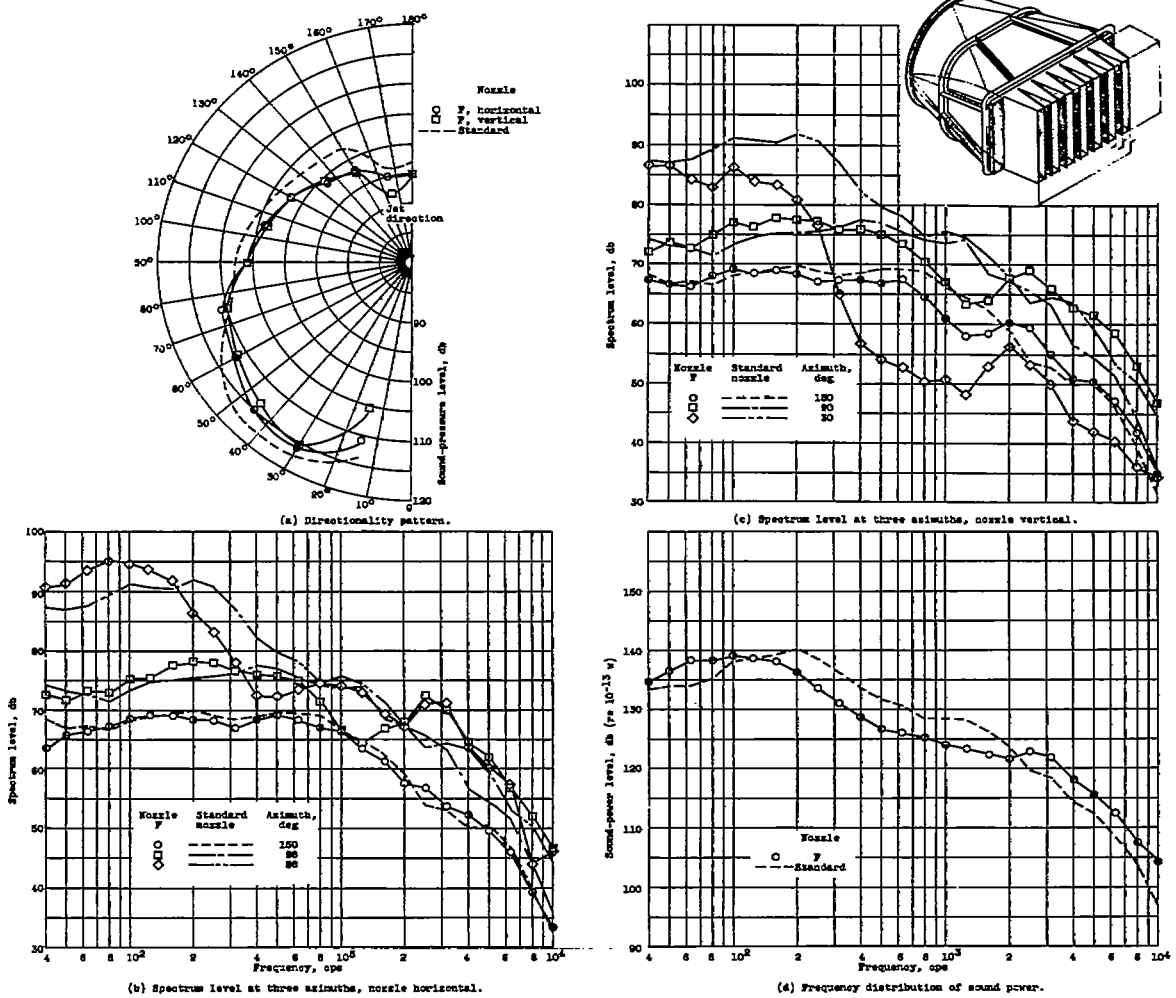


Figure 19. - Sound-field characteristics of nozzle F.

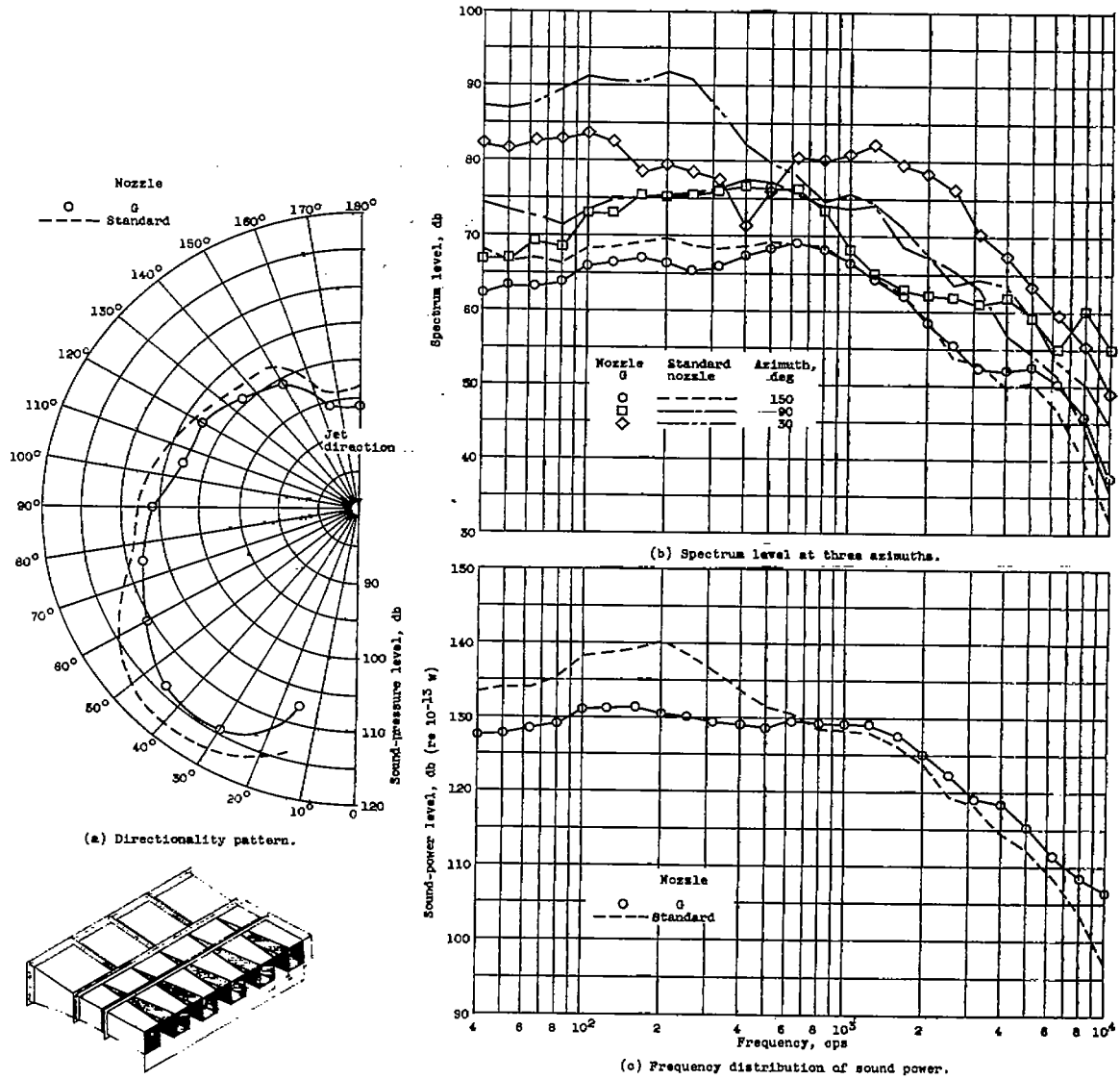


Figure 20. - Sound-field characteristics of nozzle G.

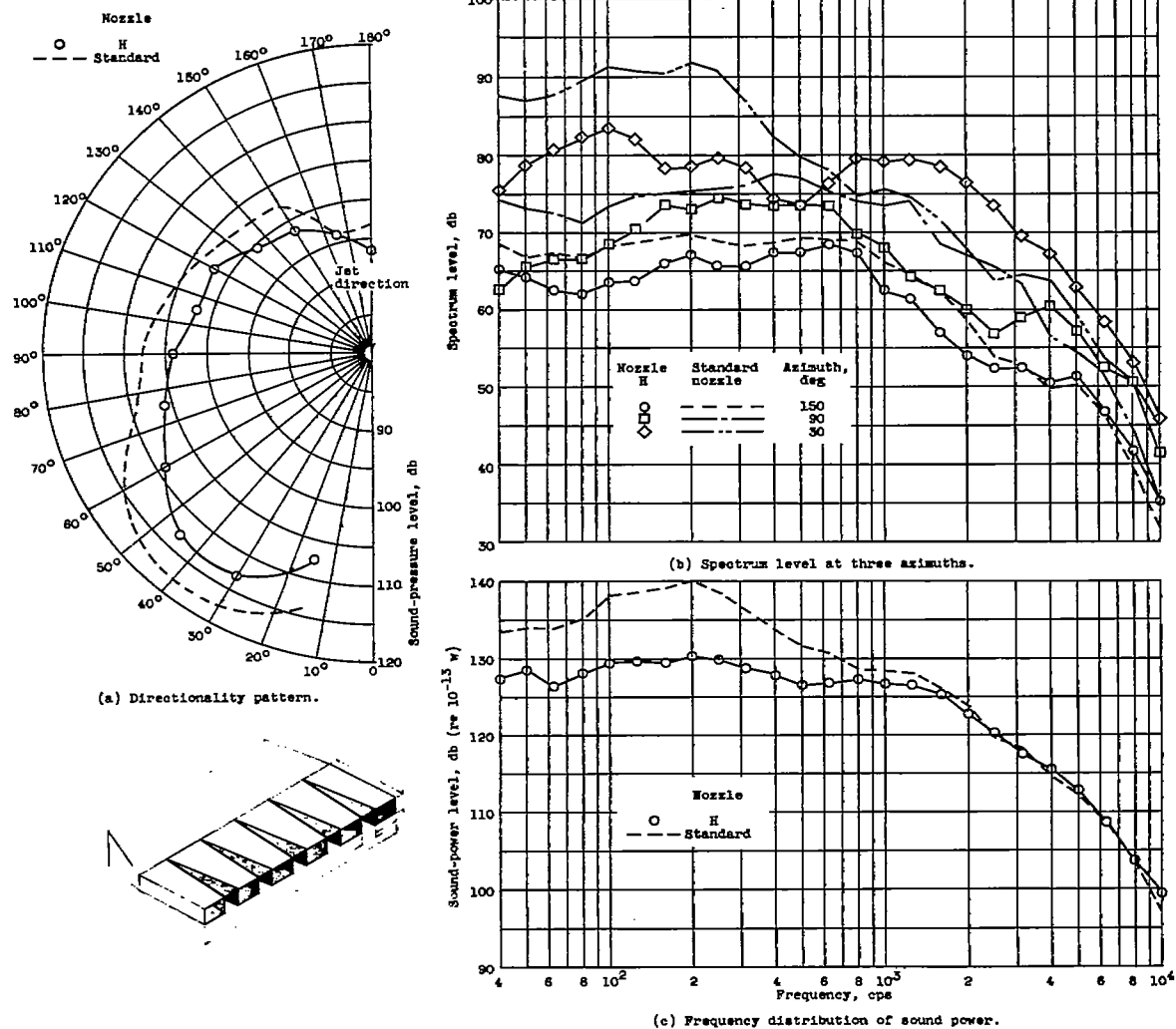
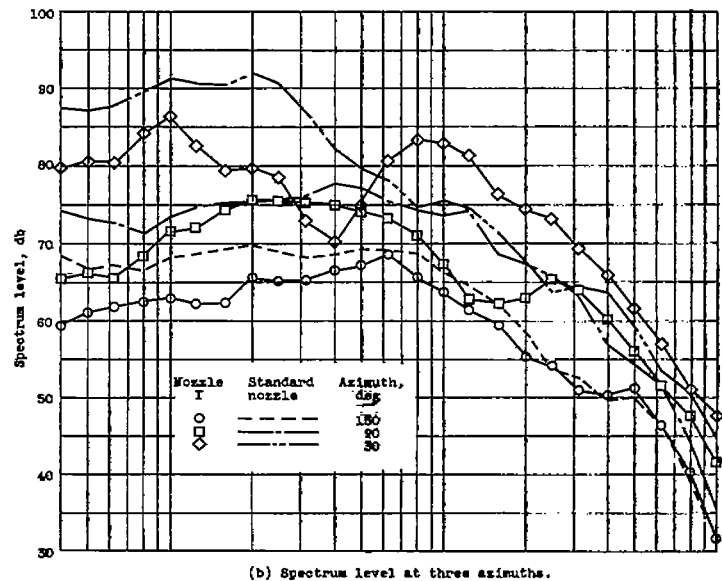
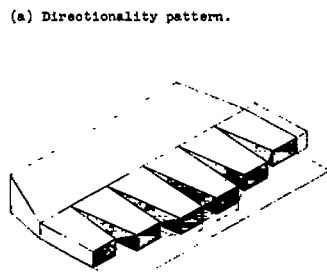
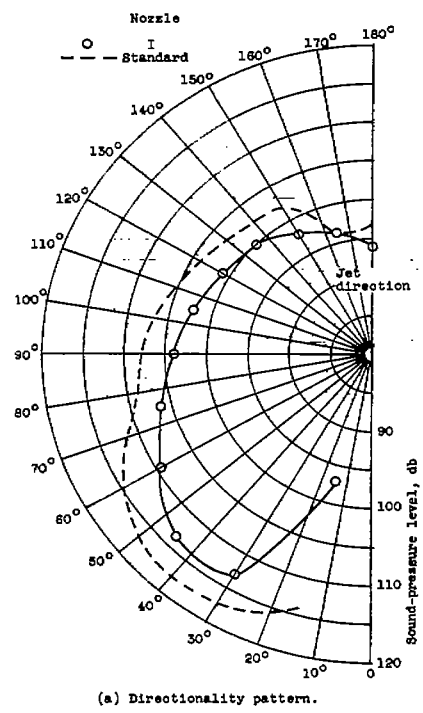
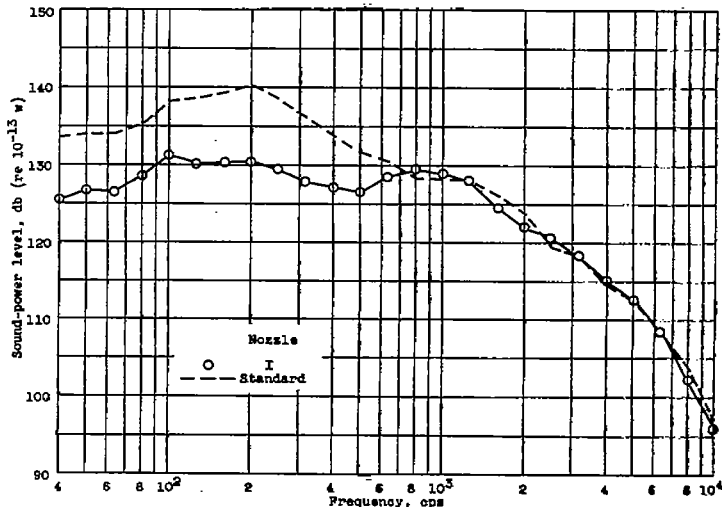


Figure 21. - Sound-field characteristics of nozzle H.



(b) Spectrum level at three azimuths.



(c) Frequency distribution of sound power.

Figure 22. - Sound-field characteristics of nozzle I.

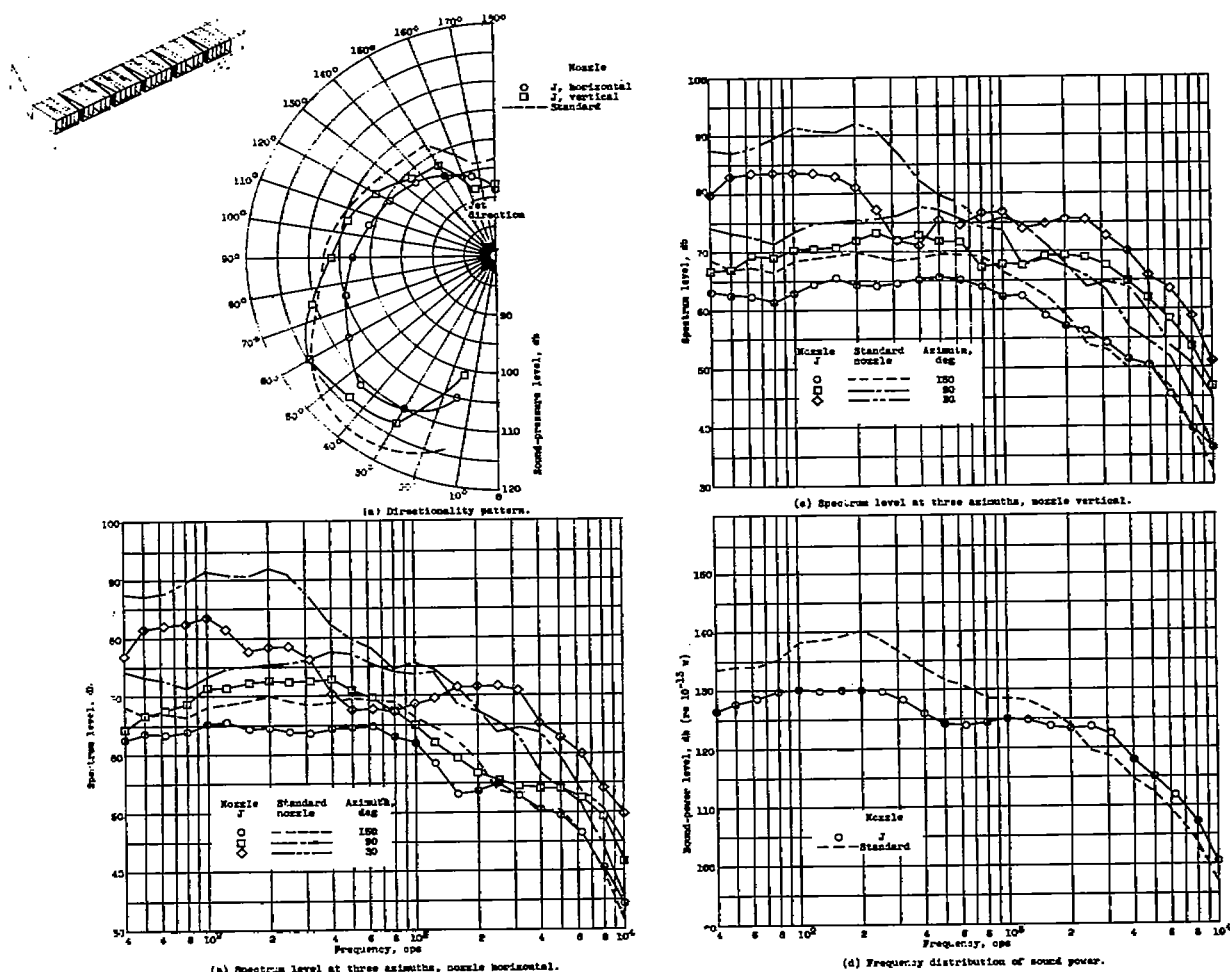


Figure 23. - Sound-field characteristics of nozzle J.

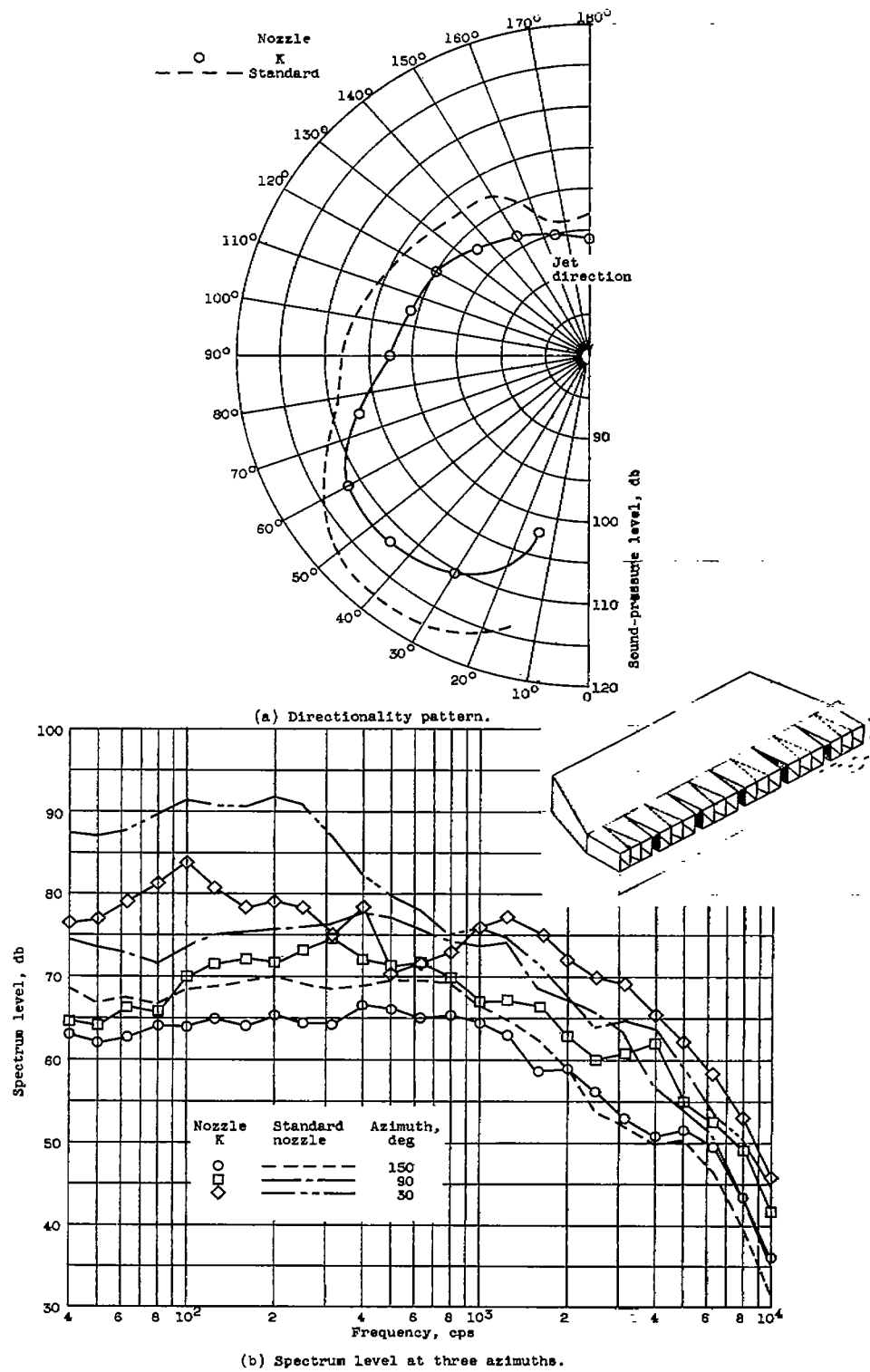


Figure 24. - Sound-field characteristics of nozzle K (nozzle horizontal).

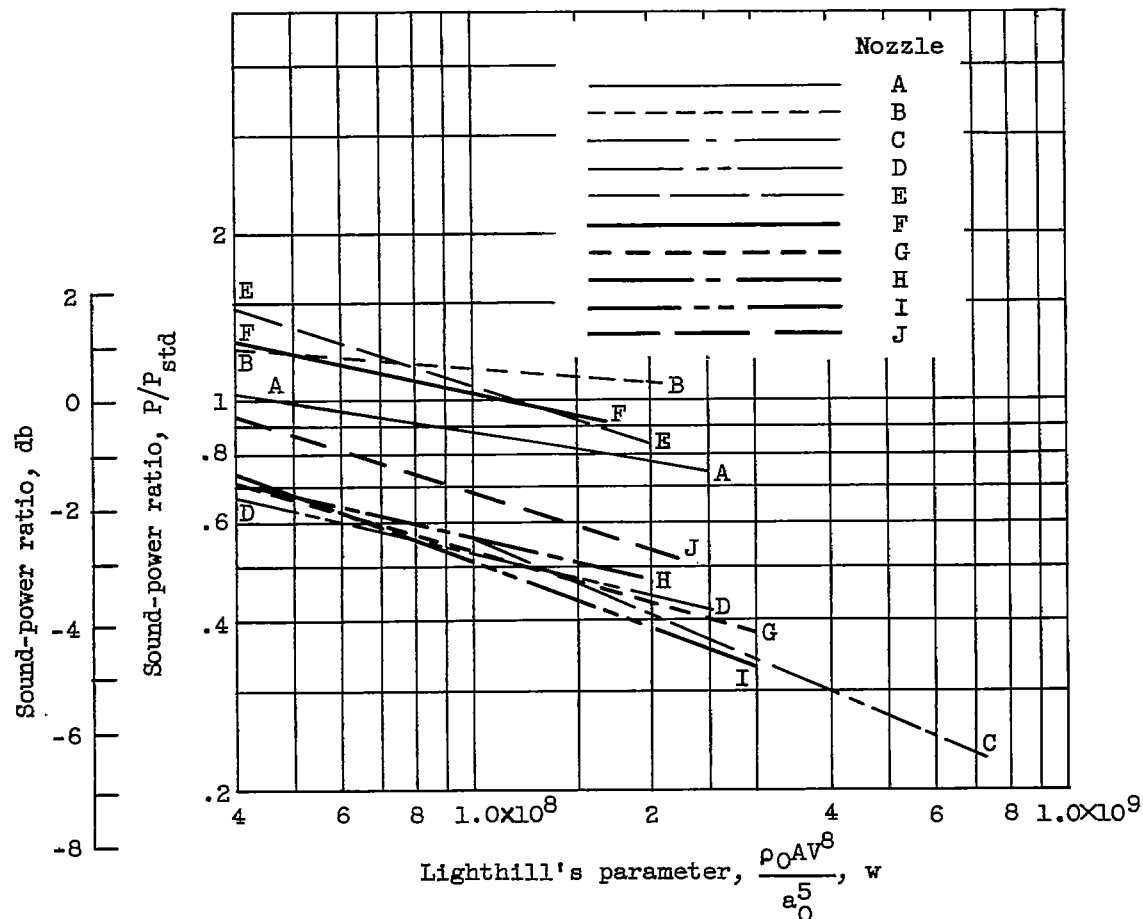


Figure 25. - Sound-power ratio as function of Lighthill's parameter.

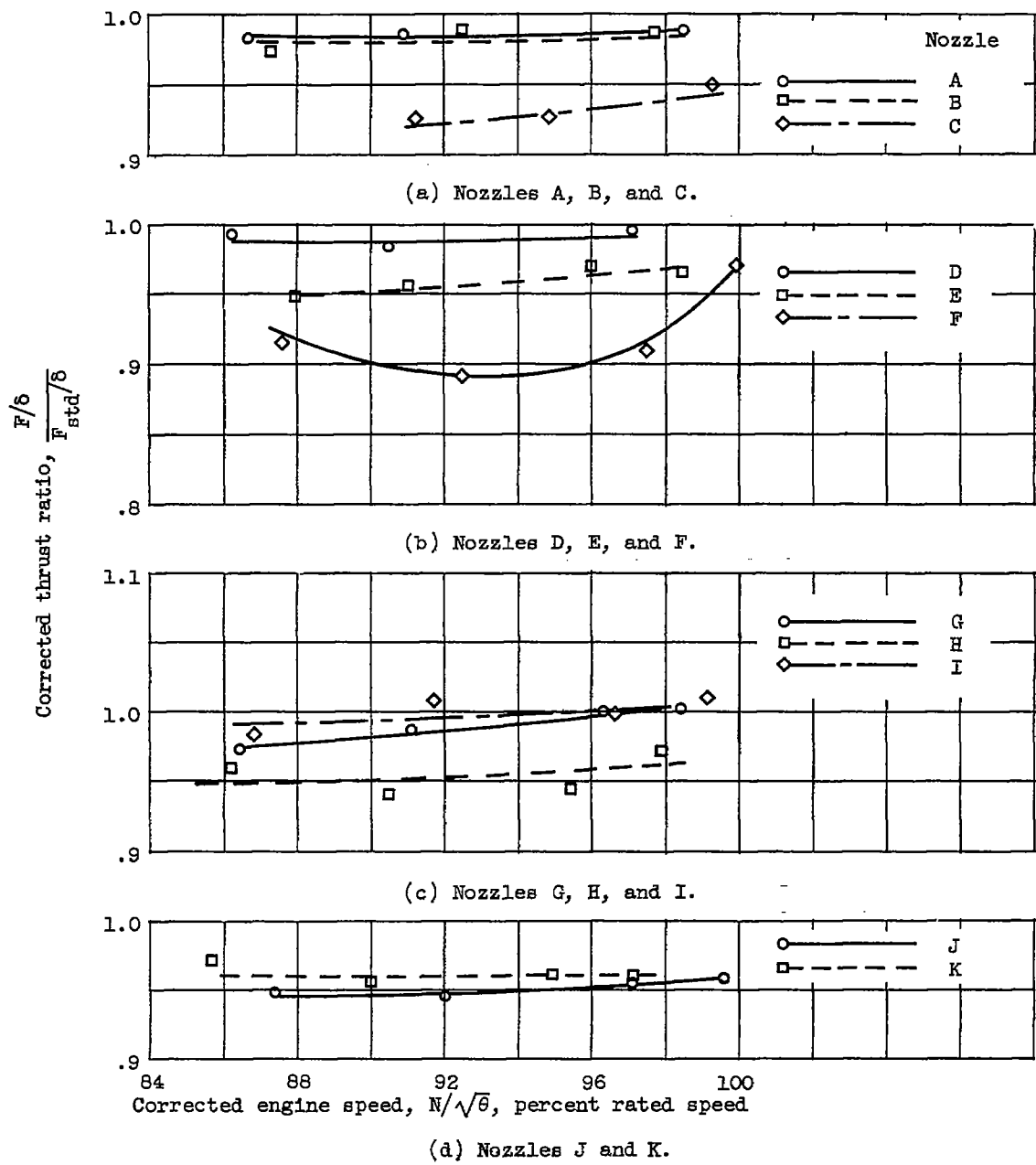


Figure 26. - Thrust ratio as function of corrected engine speed.

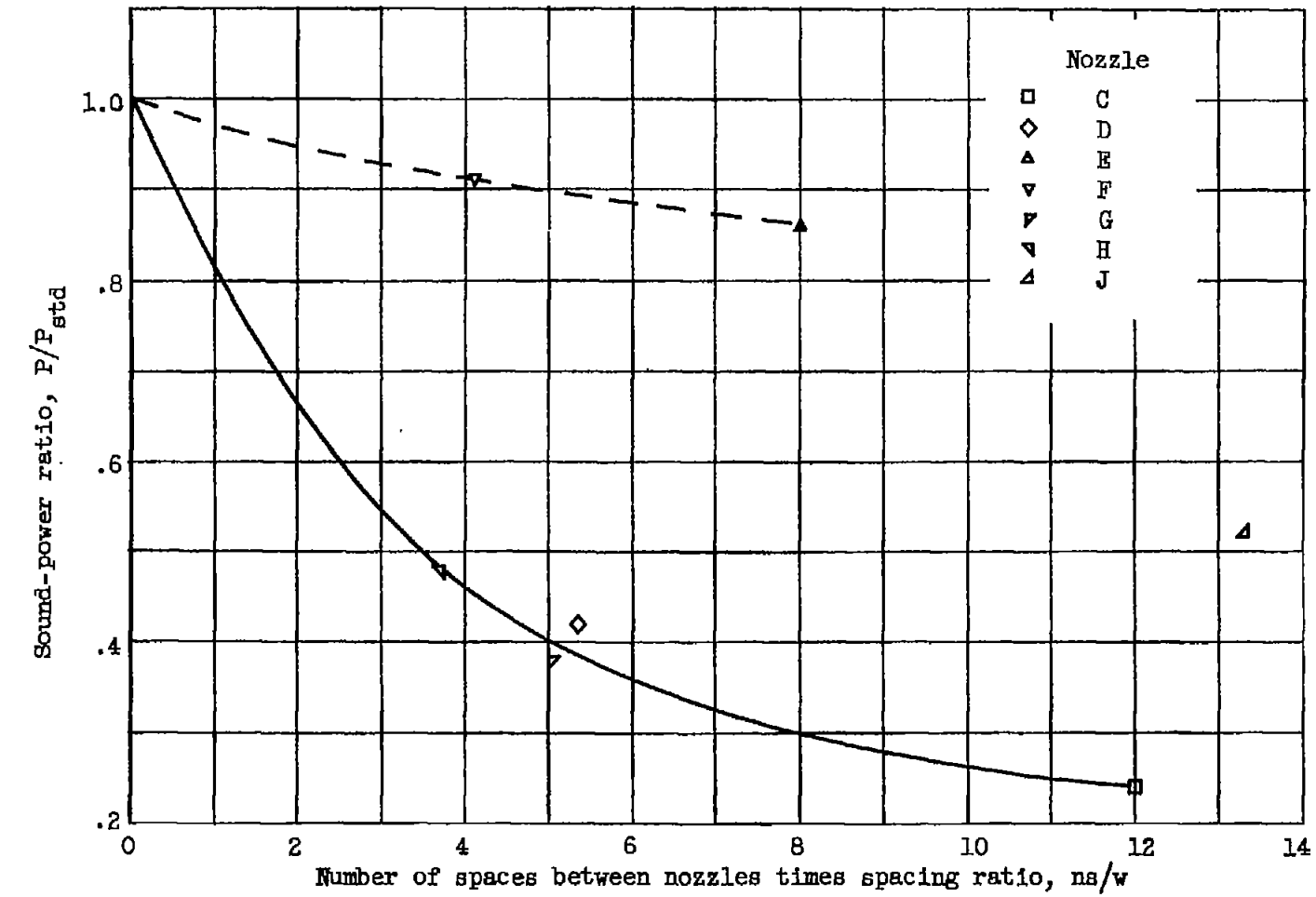


Figure 27. - Sound-power ratio at rated engine conditions as function of  $ns/w$ .